A. P. Mikitchuk, E. I. Girshova, V. V. Nikolaev, Current state of the research on optoacoustic fiber-optic ultrasonic transducers based on thermoelastic effect and fiber-optic interferometric receivers,
Компьютерная оптика, 2023, том 47, выпуск 4, 503–523

Current state of the research on optoacoustic fiber-optic ultrasonic transducers based on thermoelastic effect and fiber-optic interferometric receivers

A.P. Mikitchuk [1], E.I. Girshova [2], V.V. Nikolaev [2]
[1] Belarusian State University, 220030, Minsk, Belarus Niezaliezhnasci Avenue 4;
[2] Submicron Heterostructures for Microelectronics Research and Engineering Center of the RAS, 194021, St Petersburg, Russia Politekhnicheskaya, 26

Abstract

The work is devoted to an overview of the current state of optoacoustic fiber-optic ultrasonic transducers based on thermoelastic effect and fiber-optic interference receivers, its scope, technologies and materials used, the advantages and disadvantages of different methods and the prospects for the development of the industry.

Keywords: optoacoustics, ultrasonic devices, optical fiber, optoacoustic reciever, optoacoustic transducer.

Citation: Mikitchuk AP, Girshova EI, Nikolaev VV. Current state of the research on optoacoustic fiber-optic ultrasonic transducers based on thermoelastic effect and fiber-optic interferometric receivers. Computer Optics 2023; 47(4): 503-523. DOI: 10.18287/2412-6179-CO-1224.

Introduction

To date, ultrasonic devices are widely used in various engineering approaches, for example, in technical diagnostics [1 – 4], mixing solutions [5], cleaning and disinfection [6], and in biomedical research [7, 8]. Most often, traditional piezoelectric electroacoustic transducers are used as emitters and receivers of ultrasound. Such devices are reliable and have a long history of successful use, but they have some drawbacks. They are characterized by a high supply voltage, massiveness, high sensitivity to electromagnetic interference, and a relatively narrow frequency band [3]. A promising direction for technical applications is the development of optoacoustic methods for receiving and generating ultrasound.

Optoacoustic transducers based on thermoelastic effect are a very attractive alternative for generating ultrasound because they rely on the expansion effect of an optical absorbing layer heated by laser pulses on continuous wave radiation. Due to thermoelastic effect, the active medium is heated and cooled, which leads to a cyclical alternation of expansion and contraction, which generates acoustic waves in the environment. The principle of operation of the optoacoustic transducer is shown in Fig. 1 on the example of an optoacoustic generator based on a structure with a Tamm plasmon. Note that structure shown is presented for the case of forced acoustic oscillation at a frequency determined by the excitation optical signal modulation.

Interferometric optoacoustic receivers have an operating frequency bandwidth at the level of the best samples of similar piezoelectric devices, and surpass them in compactness and sensitivity. An optoacoustic ultrasonic generator can even be placed at the end of the optical fiber. At the same time, methods for receiving acoustic signals by fiber-optic optoacoustic devices are considered to be sufficiently developed [9], but the problem of generating broadband ultrasound using compact devices has not been fully resolved [7].

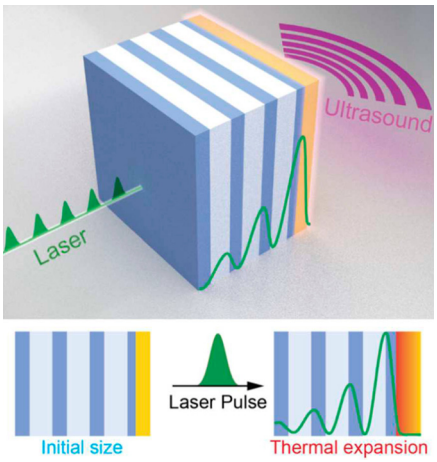

Fig. 1. Schematic diagram of the operation of an optoacoustic generator based on a structure with a Tamm plasmon [81]

The optoacoustic effect was discovered by A. Bell in 1881 and then described in the works of W. Röntgen and D. Tyndall. But at the end of the 19th century, ways of applying this discovery were not found. Studies of this physical phenomenon were not carried out for many years, resuming only with the advent of lasers. In 1962, independently of each other, A. M. Prokhorov's group in the USSR and White's group in the USA discovered the effective excitation of ultrasound in a condensed medium under the action of laser pulses. Now the potential application of the effect was obvious. First of all – hydroacoustics. In 1964, a patent was registered for an acoustic generator by Brever and Rickhoff with the idea of using the focus region of a powerful laser beam as a pulsed laser source of intense sound vibrations with a high coefficient of conversion of optical energy into sound energy. The pressure signal level reached by the authors above 0.1 MPa allowed them to propose this

source both for technological applications and for studying the ocean floor. To date, the results of both observations of the effect and the results of various applications have constituted an extensive bibliography.

Systematic studies of fundamental issues of optoacoustics in USSR were started in a coordinated manner in 1973 by teams led by professors L.M. Lyamshev [10] and K.A. Naugolnykh [11] (Academician N.N. Andreev Acoustic Institute), professor F.V. Bunkin (Physical Institute named after P.N. Lebedev), professors S.A. Akhmanov and O.V. Rudenko (Moscow State University named after M.V. Lomonosov) [12].

The most significant results abroad in the field of optoacoustics were obtained at the IBM Research Laboratory [13], Brown University [14], the Max Planck Institute [15], the University of Tokyo [16], the ETH Zurich [17] and other centers.

An urgent task, both in practical and theoretical terms, is the development of miniature optoacoustic emitters based on nanostructures. Studies show that such devices will significantly expand the operating frequency band, reduce size and weight, and implement galvanic isolation. Thus, not only will a number of limitations of traditional sources be eliminated, but the applicability scope of the device in more difficult operating conditions will be expanded: powerful radiation, high temperature.

Typically, the absorptive nanostructure is illuminated by ultrashort laser pulses (for example, femtosecond or picosecond), which excite the nanoparticle eigen acoustic oscillations (the principle is similar to a tuning fork). In this case, parameters of pulse practically do not influence the output frequency, because it is determined by the structure dimensions and sound velocity. In accordance with a newer principle, nanoparticles (NPs) or other absorbing structures are illuminated by intensity modulated laser radiation (modulation frequencies up to ~100 MHz). As a result, a change of the structure size causes the forced acoustic oscillations. Moreover, it is possible to generate a continuous acoustic sinusoid with the arbitrary frequency in the range up to ~100 MHz. Forced acoustic oscillations in the optoacouscic structure principle is similar to a speaker (loudspeaker) one: both continuous laser signals with sinusoidal modulation (to generate sinusoidal acoustic signals) and broadband pulsed signals (to generate broadband acoustic pulses) can be used.

In the case of the forced oscillations, a spatial resolution of ~10 μm is achieved and, due to low attenuation, it is possible to study structures with the size of ~1 m. In contrary, optoacoustic transducers based on eigen oscillations provide the spatial resolution less than 1 μm. However, due to large attenuation at GHz frequencies it is possible to study only rather small objects.

Tab. 1 describes the principles of acoustic oscillation excitation.

Optical intensity modulated radiation is absorbed with the characteristic time, which is much shorter than the modulation period. Due to either effect of surface plasmon resonance, or absorption in Tamm structures and etc. In this case, systems simply “repeate” external intensity fluctuations. The principle of operation of an optoacoustic transducer is that the modulated laser radiation is absorbed in the active medium of the generator, which causes a modulated change in its size and leads to the generation of acoustic oscillations. Despite the fact that research in the field of optoacoustics has been carried out at a high world level for several decades, this field of research has not yet exhausted itself. The main difficulties in creating optoacoustic converters are due to the lack of unified approaches to describing the physical mechanisms for converting an intensity-modulated optical signal into acoustic oscillations [8, 9, 18]. In the literature, relationships between the parameters of nanostructures and the characteristics of optoacoustic converters based on them are rarely given. The formation of experimental samples in the process of searching for the optimal nanostructure for such converters is resource-intensive. In light of the above, it is necessary to make computer simulation at the stage of planning an experimental study as informative and accurate as possible [19, 20]. In this regard, the establishment of relationships and patterns associated with the mechanism of optoacoustic generation will allow in the future to create more energy efficient devices.

Tab. 1. Principles of acoustic oscillation excitation

Frequency range	GHz	MHz
Operation principle	Nanoparticle acoustic oscillations at their eigen acoustic frequency (~ sound velocity / nanoparticle size)	Nanoparticle forced acoustic oscillation at a frequency determined by the excitation optical signal modulation
Energy source	Ultrashort optical pulses (e.g. femtosecond)	Intensity modulated optical signal, pulse modulation is not obligatory condition, continuous wave is also possible
Particle heating	Non-equilibrium thermal state inside the nanoparticle	Quasi-equilibrium thermal state inside the nanoparticle
Resolution and distribution length	Low range, high resolution	Long range, low resolution
Arbitrary waveform generation ability	no	yes
Example	Tuning fork (“pure” sound at its eigen frequency)	Speaker (transformation of electrical vibrations into the displacement of the membrane).

1. Application of optoacoustic devices

The rapid development of research in the field of nanostructured materials for fundamental and applied sci-

ence, in particular, for technical diagnostic systems, is explained by the fact that as the characteristic dimensions of the constituent parts decrease to the nanolevel, the structures acquire new properties due to quantum size effects and the increasing role of surface atoms and their interactions [21, 22]. In the world scientific literature, when studying the properties of various nanostructures, great attention is paid to quantum size effects. Nevertheless, the vast majority of practically implemented technical diagnostic systems based on nanostructures use surface effects due to a strong increase in the role of surface atoms, for example, atoms of nanoparticles [23, 24]. Such applications include, for example, devices for determining the change in the refractive index of liquids [25, 26], solids [27, 28], gases [29], the study of technological media [30, 31]; devices for high-temperature ultrasonic diagnostics of metal plates [32 – 34]. Therefore, the effects of the interaction of nanostructures with electromagnetic radiation are studied, taking into account the influence of the surface of the structure, as well as the thermal and mechanical processes associated with them.

Both in engineering flaw detection and in medical diagnostics, the choice of a physical diagnostic tool is of particular importance, which will allow you to identify the exact coordinates of a particular defect, violation of the structure or composition of a substance, including critical ones. Reliable diagnostics can help in time to eliminate the malfunction or even prevent an accident. Technical diagnostics, for example, includes non-destructive ultrasonic testing as a widely used reliable class of systems for flaw detection of technical objects, which has important advantages [4, 9, 19]:

1. high sensitivity to the most dangerous defects such as cracks;
2. the ability to control without stopping and disrupting the process;
3. the ability to conduct control without damaging the object under study;
4. the ability to control products from a variety of materials;
5. low cost;
6. safety for humans (unlike, for example, X-ray defectoscopy).

Modern medical diagnostics and flaw detection cannot be imagined without the use of ultrasound technologies. In medicine, ultrasound is an accessible, safe, non-invasive, highly informative method of soft tissue imaging [35 – 37]. Also, ultrasonic flaw detection is used on an industrial scale to control manufactured and already used structures, although the method has its limitations and disadvantages. The main problems of flaw detection are: the limited ability to control products made of high-grain metals and alloys of different steels [38 – 40], the need for close contact of the emitter with the surface of the device, and the difficulty of testing small parts [40 – 42]. If the first problem is fundamental for this technique, then the remaining two can be partially solved by miniaturizing the ultrasound source [43].

In modern medicine, ultrasound diagnostics is widely used: prenatal diagnostics, examination of soft tissues with the possibility of three-dimensional image reconstruction, examinations with the introduction of contrast agents, blood flow control, examinations of the heart and blood vessels. Currently, the development of devices that allow continuous monitoring of blood flow in patients in intensive care units (continuous wave doppler) is of great interest [44, 45]. In addition to the already listed advantages of ultrasound diagnostics (accessibility, accuracy, speed, safety for the patient and operator), it should be noted that an important advantage of the method is the ability to directly study moving structures (heart tissue, blood flow in the vessels). The frequency range used in ultrasound diagnostics is 2 – 30 MHz. The higher the frequency, the better the resolution of the resulting image, but the less the penetration of radiation into the tissue. Therefore, miniaturization of the ultrasound source is topical for studying small structures [46]. The practical aspects of the use of ultrasound in high-tech medical procedures are expanding every year. Today, ultrasonic generators are used not only for diagnostic and cosmetic purposes, but also in such high-tech and urgent interventions as gene therapy [47], transfer of drugs through the meningoencephalitic barrier [48], virtual biopsy of neoplasms [49]. New applications pose new challenges to instrument performance: spectrum width, power, robustness must be matched to the task at hand.

At the moment, optoacoustic communication systems are being developed quite actively [50], allowing, for example, communication between an aircraft and an underwater submarine [51] or transmitting sound over short distances "right in the ear" of an object without a receiving device [52].

Sound transmission methods without a transducer are based on the fact that water vapor is always present in the atmospheric air, and can absorb laser radiation. The modulation of the absorbed radiation makes it possible to obtain modulated mechanical oscillations of the gas in the desired region. Another important way of applying optoacoustic methods is optoacoustic spectroscopy. This technique has many important applications: non-destructive study of a chemical objects [53], including a biological one [54], control of the content of ozone in the atmosphere or carbon dioxide [55], detection of toxic substances and their traces [56]. The same approach can be used in high-tech medicine to detect target proteins [57].

A separate and relevant application of ultrasound in the life of modern society is disinfection, more relevant than ever in light of the danger of the emergence of antibiotic-resistant bacteria and the large number of circulating viruses. Ultrasonic disinfection is used in medicine [58], sanitation [59], and veterinary [60]. A big plus is that microorganisms do not acquire resistance to this type of cleaning. It has also been shown that the combination of classical disinfection techniques with ultrasonic disinfection improves the quality of cleaning objects with small cavities and tubes [61].

Thus, the field of application of ultrasonic technologies in our life is constantly expanding.

2. Optoacoustic ultrasonic receivers

The undeniable advantages of optical fiber, such as small size, dielectric design, flexibility, low losses for an intensity-modulated optical signal, and the use of bidirectional propagation, allow the use of fiber optic devices in the detection of ultrasonic vibrations [9]. Fig. 2 shows a diagram of a fiber-optic ultrasonic receiver, in which a fiber-optic probe with a Fabry-Perot interferometer at the end of the optical fiber is used as an ultrasound detector [61].

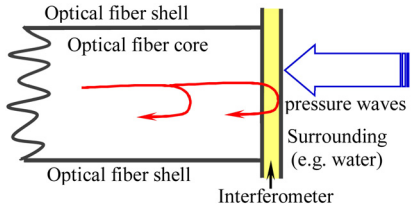

Fig. 2. Fiber-optic ultrasonic receiver, in which a fiber-optic probe with a Fabry-Perot interferometer at the end of the optical fiber is used as an ultrasound detector [62]

Ultrasonic vibrations act on an interferometer consisting of two mirrors (with reflectances of 30 % and 95 %) separated by a polymer layer 23 μm thick. The pressure wave modulates the thickness of the interferometer, which, in turn, leads to a change in natural frequencies, the position of which is determined by relatively small tuning of the laser generation frequency. A fiber-optic ultrasound receiver based on a Fabry-Perot resonator makes it possible to detect sound pressures of less than 0.1 kPa at an operating frequency band of 20 MHz, when the equivalent spectral density of the noise sound pressure is more than 0.022 [62].

To increase the sensitivity of such ultrasound receivers, it was proposed to use high-quality optical ring microcavities [63], which make it possible to detect signals in air at an equivalent spectral density of noise sound pressure of 0.215, 0.041 at 50 kHz and 800 kHz, respectively, which is comparable to the best examples of commercial piezoelectric transducers [62].

It is important to note that there are still a number of sufficiently detailed principles for receiving ultrasound using optical fiber devices [63, 64]. Some samples of fiber-optic receivers have been brought to prototypes, for example, a receiver based on the detection of mechanical deformations of an external fiber laser cavity [64, 65]. The constructed images of a test two-dimensional targets and a three-dimensional structure of two hairs were experimentally obtained using fiber-optic optoacoustic receivers, and demonstrates the possibility of resolving details with a size of less than 3 μm [66].

In a laser with an external cavity, a change in the phase shift due to the surface vibration caused by the passage of ultrasonic waves leads to a change in the laser generation frequency with time, and a time resolution of less than 100 ps is achieved [63]. Such fiber optic receivers can be used for diagnostics in aggressive environments and at high temperatures due to the high chemical and thermal stability of the optical fiber [66]. Tab. 2 contains information about the characteristics, such as band width, size and equivalent pressure of ultrasonic receivers built on various physical principles.

Tab. 2. Characteristics of ultrasonic receivers built on various physical principles

Type	Sensor size	Sensitive element size	Design	Bandwidth (MHz)	Equivalent pressure	Reference
Piezoelectric receiver	diameter > 0.5 mm	coinside with sensor size	circle, ring	50	10 kPa	[67],[68]
	diameter 0.4 mm, thickness 2 μm		circle	80	-	[69]
	diameter 0.5 mm		circle, cylinder, ring	> 25	55 kPa	[70]
Volume optics	-	-	dot, circle	5 и 20	35 Pa и 275 Pa	[71]
	-	diameter 90 μm	cylinder	17.5	100 Pa*	[72]
	-	diameter 90 μm	cylinder	-	130 Pa*	[73]
	-	-	dot, circle	25	20 kPa	[74]
Fiber optics	diameter 125 μm	diameter 8 μm	cylinder	50	92 kPa*	[75]
	diameter 125 μm	diameter 8 μm	cylinder	50	4.18 kPa*	[76]
	diameter 125 μm	diameter 8 μm×100 μm	cylinder	20	0.45 kPa	[77]
	diameter 125 μm	diameter 8 μm	cylinder	50	9.2 kPa*	[75]
	diameter 125 μm	thickness 10–40 μm	dot	20	< 1 kPa	[77]
Microresonators integrated with optical fiber	500 μm, thickness 0.5 mm	2×1.5 μm^2	cylinder	20	100 Pa	[78]
	500 μm, thickness 0.5 mm	1.5×1.5 μm^2	cylinder	60	6.5 kPa	[79]
	diameter 60 μm, thickness 250 μm	0.8×0.8 μm^2	ring	140	6.8 Pa	[80]

It can be seen that ultrasound receivers built on the basis of fiber optic and microresonators at the end of an optical fiber have characteristics in terms of the operating frequency band at the level of the best examples of receiving piezoelectric transducers, and in terms of compactness and low value of the equivalent noise pressure, it

is significantly surpass them. The problem of receiving ultrasound, even with the help of compact fiber-optic devices, is not acute [67], on the contrary, the greatest difficulties arise when it is necessary to emit ultrasound with frequencies above several megahertz from small sources with sizes less than 300 μm.

One can see that optoacoustic ultrasonic receivers allows all-optical detection of acoustic waves for very different situations under study. They allow to receive acoustic signals with frequencies up to 140 MHz with the effective sensor size less than 100 μm. The analysis of the set of papers shows that this topic is rather developed. It is not in the area of scientific, but technical problems.

3. Optoacoustic transducers

During the existence of this technique for generating ultrasonic waves, a large number of different materials, including hybrid ones, have been tried as an active medium for optoacoustic emitters. The first active media of the emitter were ordinary metal layers, which was a logical and intuitive solution, since the metal absorbs radiation well. But the high ability of the material to absorb optical radiation is only the first step towards highly efficient energy conversion. Metals do not have a high coefficient of linear thermal expansion, therefore their expansion under heating, the severity of which determines the amplitude of the generated mechanical vibrations and, accordingly, their energy is significantly less than it could be when other materials are heated.

In general case, the efficiency of thermoelastic conversion of light energy into sound when using eigen oscillations is determined by the Grüneisen parameter of the light-absorbing medium, as well as the ratio of the acoustic impedances of the absorbing medium and the medium in which it is required to create a sound field [81, 82]. On the other words, from the point of view of the environment, it is necessary, firstly, the ability to absorb, and secondly, suitable thermoelastic and mechanical parameters. The adequacy of the use of one or another active medium can be assessed using the Grüneisen parameter. The Grüneisen parameter can serve as a criterion for the adequacy of using a material as an active medium of an optoacoustic transducer [82]. It is a dimensionless parameter that describes the effect of a change in the volume of a crystal lattice on its vibrational properties and, as a consequence, the effect of a change in temperature on the size or dynamics of the lattice. Additionally, thermooptical sound excitation efficiency is therefore proportional to the light radiation power [82]. In terms of radiation, the higher its power, the higher the efficiency, so lasers are used as a source and optoacoustics had practically no engineering applications before their invention.

Strictly speaking, the efficiency of optoacoustic conversion (we are talking about the thermooptical mechanism of generating ultrasound) is determined by the parameters of the exciting optical radiation and the active medium. Note that for a special case of multilayer nanostructures, the authors demonstrate additional way of estimation based on finite difference method [83]. For example, in the even case, the following formula can be used to express the degree of increase in the thickness of the absorbing layer of a multilayer nanostructure upon absorption of laser pulses [83]

$$B \sim \varepsilon G/(c\rho), \quad (1)$$

where B is the increase in active layer thickness, c and ρ are the specific heat capacity and density of the active media material and ε is it's thermal expansion coefficient. In the light of the foregoing, it would be logical to add a material with a high coefficient of thermal expansion to the heating metal. An excellent material in this regard is polydimethylsiloxane and some other organic compounds. However, a high coefficient of linear thermal expansion of the active medium material does not in itself guarantee a high energy efficiency of the device. To obtain a significant amplitude of mechanical oscillations of the sample surface, it is necessary that the temperature has time to relax between the absorptions of two pulses.

When modeling thermal expansion, Tamm structure is not considered as free. The thermal and elastic properties the spatially fixed substrate as well as the environment surrounding are taken into account. Moreover, when modeling and solving structural analysis problems, appropriate boundary conditions are applied.

Unfortunately, polydimethylsiloxane and other polymers with high thermal expansion coefficients are a good heat insulator, which limits the maximum operating frequency of a potential device. Fig. 3 show the time and spatial distribution of temperature in the structure of an optoacoustic transducer. Since the power of sound emitted by an oscillating surface is proportional to the square of the oscillation amplitude, it would be advisable to ensure maximum cooling of the structure after the end of the heating pulse, ideally to the initial level, which can be achieved either by increasing the thermal conductivity of the metal layer or by reducing the repetition frequency.

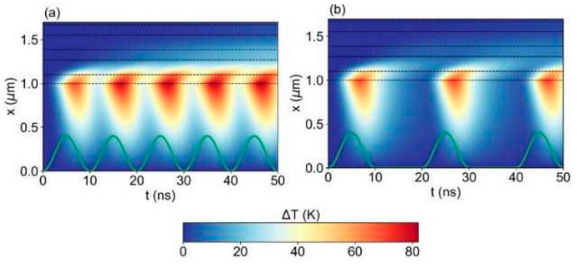

*Fig. 3. Temporal and spatial distribution of the temperature increase Δ(x, t) under periodic heating of the structure (a) with sinusoidal modulation of the laser power I(t) with frequency 100 MHz, and average flux density I(t) =10⁶ W/cm²; (b) with a sequence of sinusoidal pulses with duration of 10 ns and repletion rate 50 MHz, and average flux density I(t) =5*10⁵ W/cm² Green line show the temporal dependence of laser flux density I(t)*

For the reasons listed, it becomes clear that in addition to high absorption in the structure at the laser wave-

length and a high coefficient of linear thermal expansion of the active medium, it is also necessary to ensure adequate heat removal from the structure for adequate cooling between pulses. The figure shows the time dependence of the surface coordinate of a structure sample with a Tamm plasmon upon irradiation with pulses of different frequencies. It can be seen that as the frequency increases, the system ceases to adequately relax and energy efficiency is significantly reduced due to this. Very important to note that this condition is necessary in realize forced acoustic oscillations.

Most organic compounds with high thermal expansion are actual heat insulators, that is, once heated and expanded, they will not have time to cool down to generate stable mechanical disturbances. Over the past decade, many ways have been proposed to combine all the above requirements for the active medium on the base thermoelastic mechanism of an ultrasound generator, and modern devices are several orders of magnitude more energy efficient than the first samples, which are thin metal plates.

All active media for thermoelectric acoustic wave excitation can be divided into two large groups: classical bulk absorbers and nanostructured samples. It has been experimentally shown that, in order to increase the efficiency of an optoacoustic source of ultrasound, instead of uniform absorbing films at the end of an optical fiber, it is possible to use composite layers, for example, based on graphite [83]. Such layers have higher optical absorption, lower reflectivity and high thermal stability. As a thin absorbing layer, it is possible to use a monolayer of metal NPs with an intense SPR maximum in the optical absorption spectrum, structures with a Tamm plasmon. In the general case, the SPR frequency is determined by many factors: the material, the size and shape of the nanoparticles, the mutual arrangement of the nanoparticles, as well as the material parameters of the substrate and the environment.

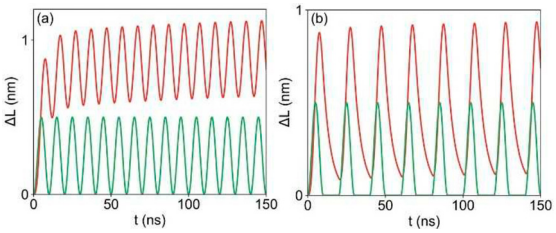

*Fig. 4. Oscillation of the surface of the structure with Tamm plasmon during heating by laser (a) with sinusoidal modulation of the laser power (t) with frequency 100 MHz, and average flux density I(t) =10^6 W/cm^2;, (b) with a sequence of sinusoidal pulses with duration of 10 ns and repletion rate 50 MHz, and average flux density I(t) =5*10^5 W/cm^2.Green line show the temporal dependence of laser flux density I(t)*

The use of nanostructures in the form of a monolayer of nanoparticles as an absorbing medium at the edge of an optical fiber allows:

1) to realize a high absorption coefficient of the incident laser radiation, which is achieved due to the SPR effect;
2) to provide a wide band of operating frequencies by minimizing the thickness;
3) to ensure high photoresistance, since optical radiation does not cause degradation of the absorbing layer of noble metal NPs, semiconductor and metal layers in the case of a structure with a Tamm plasmon.

The maximum frequency of the generated ultrasonic signal significantly depends on the thickness of the absorbing layer. Despite the fact that for the two most common applications of ultrasonic waves, medical diagnostics and industrial flaw detection, the required range is usually 2 – 30 MHz, but more modern and developing technologies (ultrasonic spectroscopy, materials science applications, high-tech medicine) require ever higher resolutions and frequencies every year. Therefore, to expand the field of application of optoacoustics, it is necessary to ensure the absorption of incident laser radiation in the thinnest possible layer of an optoacoustic transducer, which is facilitated by the use of thin-film and nanostructured systems.

A large number of publications are devoted to the experimental creation of optoacoustic converters based on forced acoustic oscillations, but there is no full-scale optimization of the structure parameters at the stage of experiment preparation. References to publications are given with a brief description in Tab. 3. Note that in this paper, acoustic wave excitation is studied in the case of liquids and gases. The analysis is also complicated by the fact that there is no single standard for assessing the energy efficiency of a device, since the efficiency of converting optical energy into mechanical energy depends on frequency.

At the moment, the world scientific community has already accumulated enough knowledge about the physical processes underlying optoacoustic conversion. The main problem currently standing between us and really high-performance devices with wide operating frequency bands is that the energy conversion process has many parameters, which significantly complicates its optimization. For example, the combination of a metal and a polymer in the hybrid material of the active medium of an optoacoustic transducer to combine their "useful" properties (the ability to absorb laser radiation and high thermal diffusivity for a metal and a high coefficient of linear thermal expansion for a polymer) always leads to the appearance in the final material of "harmful" properties of the components. Just as already mentioned, the influence of various factors depends on the operating frequency: if at low frequencies the heat-insulating properties of polymers interfere slightly, then as the frequency increases, their influence becomes fatal and the energy conversion efficiency becomes even lower than for a simple metal layer.

Indeed, the frequency range is determined by a whole set of parameters. However, in the case under study we are talking about the excitation of forced acoustic oscillations, when the thermal relaxation of the absorber turns out to be a much faster process compared to the modulation of external optical signal. Typically, the absorptive nanostructure is illuminated by ultrashort laser pulses

(for example, femtosecond or picosecond), which excite the nanoparticle eigen acoustic oscillations (the principle is similar to a tuning fork). In this case, parameters of pulse practically do not influence the output frequency, because it is determined by the structure dimensions and sound velocity. In accordance with the newer principle, nanoparticles (NPs) or other absorbing structures are illuminated by intensity modulated laser radiation (modulation frequencies up to ~100 MHz). Optical intensity modulated radiation is absorbed with the characteristic time, which is much shorter than the modulation period. Due to either effect of surface plasmon resonance, or absorption in Tamm structures and etc. As it mentined previously, forced acoustic oscillations in the optoacouscic structure principle is similar to a speaker (loudspeaker) one: both continuous laser signals with sinusoidal modulation (to generate sinusoidal acoustic signals) and broadband pulsed signals (to generate broadband acoustic pulses) can be used. In the case of the forced oscillations, in this case, systems simply "repeate" external intensity fluctuations. On the other words, the active structure is under full control of the external signal. As a result, such structures are rather slow in comparison even with the level of 1990s [81, 82].

Tab. 3 shows comparative characteristics of ultrasonic optoacoustic emitters based on forced acoustic oscillations with different active media (fiber-optic design is highlighted by blue color). Despite the fact that metal films as an active medium are the most primitive solution, they still find application in some specific tasks. Laser printing with gel microdroplets containing certain living organisms is an emerging technology, progress in which is important for microbiology, biotechnology and medicine. The absorption of a short laser pulse in a thin metal film of the donor plate facilitates the transfer of gel microportions. During this process, pressure surges occur that can lead to damage and loss of biological material, so it is important to control them. A study was carried out: laser pulses with a wavelength of 1064 nm, an energy of 7 – 120 μJ, a duration of 4 – 30 ns, and a laser beam diameter of 30 μm were applied to Ti and Cr films of glass donor slides [85]. Experimental estimates of the emerging jumps were made on the basis of acoustic pressure measurements in the far zone in the range of 1 – 100 MHz using a hydrophone based on a lithium niobate crystal. According to the obtained data, in the working laser energy range E = 15 – 30 μJ, pressure jumps from 20 bar to 5 kbar appear on the donor wafer in a gel layer 200 μm thick when using an absorbing Ti film and from 20 bar to 10 kbar for a Cr film. The high efficiency of optical-acoustic conversion for Cr films is explained by the better adhesion of this metal to the glass surface.

As the active medium of the ultrasonic emitter, composite materials made of carbon nanotubes and polymethylsiloxane, which generate shock waves using optoacoustic technology, can be used. A thin layer of heat-conducting carbon nanotubes and polydimethylsiloxane elastomeric polymer is applied to the concave surface of a transparent polymethyl methacrylate to convert laser energy into acoustic energy using the thermoelastic effect of the composite transducer.

Efficient conversion of laser energy requires optimal use of various properties of composite transducers, in particular, the diameter. An experimental study was made of the influence of the diameter of composite transducers on the properties of shock waves [106]. It is shown that an increase in the diameter of the composite transducer and the input laser energy leads to an increase in the peak pressure of shock waves. The maximum positive and negative pressures of the generated shock waves were 53 MPa and – 25 MPa, respectively. Thus, it was shown that an increase in the size of the transducer can lead to an increase in peak pressure in situations where it is required, and an increase in the device is not critical (for example, transcranial research).

As a rule, the wavelength of the laser used is dictated by the absorption spectrum of the material of the active medium of the generator; because of this, blue-green lasers are often used. But modern nanophotonics makes it possible to create structures with high absorption at a given wavelength. Thus, a new scheme of an optoacoustic generator based on a structure with a Tamm plasmon was proposed. The structure of the proposed design provides complete absorption of the laser pulse at a predetermined wavelength, which allows the use of compact, powerful and affordable infrared semiconductor lasers with a wavelength of about 1 μm for optoacoustic generators. The characteristics of various materials were analyzed and it was shown that a structure using magnesium as a metal has the maximum efficiency. It has been established that the energy efficiency of converting light into mechanical vibrations increases linearly with increasing flux density and modulation frequency of periodic excitation.

Optoacoustic devices are used to study the brain, in particular for neuromodulation with high spatial resolution. For more accurate work with a specific neuron, a tapered fiber optoacoustic emitter (TFOE) was developed that generates an ultrasonic field with a high spatial accuracy of 39.6 μm [107]. Carbon nanotubes and polydimethylsiloxane or graphite powder are used as an active medium [108]. Precisely directed ultrasonic perturbations generated by TFOE made it possible to integrate optoacoustic stimulation with highly stable recording of the response on individual neurons. Thus, direct measurements of the electrical response of single neurons to acoustic stimulation were carried out. This technique is a non-genetic technology of unicellular and subcellular modulation.

New studies have appeared that describe lead halides perovskites as a promising material for the active medium of an ultrasonic emitter due to their thermal properties and high absorption coefficient. The phonon spectrum was theoretically calculated and it turned out that the overlap of optical phonons and acoustic phonons leads to an up-conversion of acoustic phonons and a low thermal

diffusion coefficient. The experimentally fabricated PDMS/MAPb I_3/PDMS device simultaneously provides a wide bandwidth (– 6 dB bandwidth: 40.8 MHz; center frequency: 29.2 MHz) and high conversion efficiency (2.97×10^{-2}) [109]. Such parameters of the device allow us to count on its competitiveness.

Tab. 3. Comparative characteristics of ultrasonic optoacoustic emitters based on forced acoustic oscillations with different active media (fiber-optic design is highlighted by blue color)

Absorption material (protective coating)	Structure design	Maximal acoustic pressure (MPa)	Surfase power density of excitation (mJ/cm^2)	Bandwidth (MHz)	Reference
Steel layer	Volumetric structure with diameter of 28 mm	1	~10	<1	[86]
Cr layer	Volumetric structure with diameter of 6.35 mm	0.02 – 0.03	~0.5	<1	[87]
Black acrylic pigment	Volumetric structure	~0.02	-	<1	[88]
Carbon nanotubes (Polydimethylsiloxane)	Volumetric structure with diameter of 6 mm	57	260 – 270	<1	[89]
Carbon nanotubes (Polydimethylsiloxane)	Volumetric structure with diameter of 15 mm	30	20	<1	[90]
"Black" carbon nanotubes (Polydimethylsiloxane)	Planar	0.8	~10.000	<1	[91]
Al layer with graphene oxide	Planar	~9	56	<1	[92]
Au nanoparticles (Polydimethylsiloxane)	Planar	0.0027	~20	<1	[93]
Au nanoparticles (Polydimethylsiloxane)	Planar	0.19	13	3.1	[94]
Carbon nanofibers (Polydimethylsiloxane)	Planar	12	3.7	8	[95]
Carbon nanoparticles (Polydimethylsiloxane)	Planar	4.8	3.6	21	[94]
Graphite powder	Structure deposited at the optical fiber 600 μm	0.15	~3.5	>10	[95]
Carbon nanotubes (Polydimethylsiloxane)	Structure deposited at the optical fiber 200 μm	4.5	36	15	[96]
Carbon nanotubes (Polydimethylsiloxane)	Structure deposited at the optical fiber 200 μm	4	96	20	[97]
Layer Al with graphite (Epoxy resin)	Structure deposited at the optical fiber	0.78		20	[8]
Au nanoparticles (none)	Structure deposited at the optical fiber	0.0024	~4200	<1	[100]
Au nanoparticles (none)	Structure deposited at the optical fiber	0.0016	1770	<1	[101]
Au nanoparticles (Polydimethylsiloxane)	Structure deposited at the optical fiber with size of 400 μm	0.0075	-	<1	[102]
Au nanopores (none)	Structure deposited at the optical fiber with size of 62.5 μm	0.0027	~100	7	[103]
Au nanoparticles (Polydimethylsiloxane)	Structure deposited at the optical fiber with size of 400 μm	0.037	126	2.1	[104]
Au nanoparticles (Polydimethylsiloxane)	Structure deposited at the optical fiber with size of 400 μm	0.64	8.75	>20	[105]
Au nanoparticles (Polymers)	Structure deposited at the optical fiber	Not available	Not available	57 (at – 10 dB)	[8]

Since the optoacoustic conversion process is multifactorial and is used in various technological tasks with different performance requirements, it seems logical not to look for a single universal form of the device, but to adapt its active medium to specific requirements. Due to the variety of possible materials and ways of structuring the sample, the optimization process is quite complex and multifactorial. But the first steps along this path are already being taken. For example, studies have been conducted on the optoacoustic conversion efficiency of an Au/polydimethylsiloxane (PDMS) composite [110]. The thickness of the Au layer was optimized by simulating a multiphysics process based on the Drude-Lorenz model and the finite element method. The results showed that the optimal Au thickness of the Au / PDMS composite is 35 nm. The results were verified experimentally, in addition, Au / PDMS composites were deposited on the surface of aluminum alloys, which improved the thermoelas-

tic laser ultrasonic signals by almost 100 times. A study was also carried out to supplement and optimize the structure of an ultrasonic emitter based on structures with a Tamm plasmon [111]. It was shown that the use of polydimethylsiloxane as an additional layer of the structure of an optoacoustic transducer is expedient from the point of view of increasing the efficiency of energy conversion at frequencies up to 50 MHz, and the thickness of the optimal polymer layer depends on the expected operating frequency. At frequencies of the order of several MHz, this design improvement leads to an increase in efficiency by 4 orders of magnitude. The efficiency of energy conversion for the structure with polydimethylsiloxane first increases with frequency, and then begins to decrease due to the impossibility of normal temperature relaxation. Note, with increasing frequency, the gain in energy efficiency decreases due to the fact that the structure does not have time to cool down due to the thermal insulation properties of polydimethylsiloxane. At frequencies above 50 MHz, with a given pulse energy, the structure is heated above 150 degrees Celsius, which is unacceptable for polydimethylsiloxane.

The relationship between the design of the nanocomposite and the characteristics of the optoacoustic ultrasonic transducer was investigated by modeling at several scales the behavior of the material, the response of the device, and the propagation of acoustic waves in the medium [112]. First, the effect of the size and concentration of nanoparticles on the effective properties of the composites was quantitatively investigated using the finite element analysis method. Secondly, the effective properties of the nanocomposite were assigned to the layer, which is modeled as a homogeneous material. Finally, the propagation of ultrasound in water was calculated using a theoretical wave propagation model. The prediction by the theoretical calculation was compared with the experimental data in the literature. Based on a hierarchically integrated prediction procedure, the optimal conditions for optoacoustic nanocomposites were investigated through a parametric study with particle size and concentration as variables. The results define material designs optimized for various device characteristics such as high pressure and high bandwidth.

In conclusion of this section, we would like to note once again that for high energy efficiency of an optoacoustic ultrasonic transducer, it is necessary to find the optimal combination of many system parameters, in particular, the optical and thermophysical properties of its constituent materials. The design of the device and the choice of material must simultaneously ensure:

1) complete absorption of laser radiation at a given wavelength;
2) efficient heating of the absorbting layer by laser pulses;
3) efficient heat removal from the absorbting layer to avoid overheating;
4) the maximum amplitude and the desired time dependence of the oscillations of the sample surface.

Since the process is multyparametric, it would be convenient to apply modern methods of computer algorithms, such as genetic algorithms and machine learning, to optimize the structure and select the materials included in it. This approach will make it possible to adapt the emitter to specific tasks and save time at the stage of preliminary modeling. Such ways of optimizing optical structures have already been successfully applied, for example, to the design of highly efficient ultrathin layered reflectors [113].

4. Modeling techniques for optoacoustic transducers

The variety of different combinations of materials, substrates, and environments is so great that it is impossible to carry out these studies only through experiments. Moreover, to achieve the highest absorption, it is important that the laser emission frequency be as close as possible to the spectral position of the maximum in the absorption spectrum. Additionally, test structure synthesis during the search of the optimal optoacoustic transducer design is rather expensive and long. So, it is important to use complementary experimental data and the results of modeling the optoacoustic characteristics (position, width of the spectral peak, absorbed power, duration of the heat transfer process, thermal relaxation parameters) of such structures.

The optical properties of single nanoparticles or layered nanostructures are described in terms of simple models. However, much more adequate to the experiment simulation is implemented using the numerical solution of the full set of Maxwell's equations. The variety of ways to solve a set of these equations is related to the ultimate goal of modeling. As applied to nanostructures, there are approximate analytical and numerical methods for solving Maxwell's equations with directly discretizing, both in differential and integral form. It makes it possible to model electromagnetic properties with varying degrees of accuracy [115]. The main and most frequently used approaches to the calculation of optical characteristics and the theory of optical evaluation of the nanostructure properties are given below.

The Rayleigh theory solves the problems of propagation of optical radiation in a continuous isotropic medium with spherical particles embedded in it, the dimensions of which are small compared to the wavelength of light (less than 1/10 of the wavelength of the incident radiation) and the dielectric constant is different from the dielectric constant of the environment [115, 116]. According to the theory of Rayleigh scattering, the scattering intensity is proportional to the sixth power of the NP size and inversely proportional to the fourth power of the radiation wavelength, and unpolarized light scattered at an angle of 90 degrees is completely polarized. Such a theory is applicable only for the case of homogeneous isotropic spherical nanoparticles located at a sufficiently large distance from each other (in the approximation of single light scattering), and is not suitable for describing complex nanostructures, especially near the interface.

The Mie theory, based on classical electrodynamics, describes the optical properties of homogeneous isotropic spherical NPs with a size comparable to the wavelength of the incident radiation, placed in isotropic homogeneous dielectric matrice. The Mie theory is based on the expansion of the characteristics of an electromagnetic field interacting with a spherical NP in terms of vector spherical harmonics, followed by the calculation of the coefficients of this expansion. This approach also takes in to account the effects of refraction, interference and diffraction of waves [117, 118]. The theory is an exact analytical solution to the problem of plane wave diffraction on a sphere. This uses a number of assumptions:

1. the effects of electromagnetic wave delay [119] are not taken in to account, while the phase of the wave is constant throughout the entire nanostructure [120, 121];
2. only dipole interparticle interactions (multipole oscillations of the 1st order) are taken in to account, neglecting oscillations of higher orders, such as quadrupoles, octupoles, and so on [122];
3. spherical NPs are homogeneous and isotropic, much smaller than the wavelength of the incident radiation ($r << \lambda$) [123];
4. for very small NPs, quantum size effects appear [125], and with an increase in the radius above 40 nm, a significant long-wavelength shift of the SPR band occurs, and multipole oscillations must be taken in to account for calculations.

By choosing the appropriate coordinate systems and boundary conditions, it is possible to describe NPs with a more complex shape than a spherical one. However, it turns out to be impossible to accurately describe nanostructures near the interface and extended nanostructures in the form of monolayer nanoparticles. It should be noted that, for example, for NPs larger than 40 nm the dipole quasistatic approximation gives a low accuracy in describing the optical properties. In this case, to reduce the error, it is necessary to use the quadrupole quasi-static approximation, which takes in to account interactions of higher orders.

The method of discrete dipoles makes it possible to describe the scattering of electromagnetic radiation by NP of arbitrary shape. Within the framework of this method, a nanostructure is represented as a cubic lattice of point dipoles, the polarizability of each is determined by the local refractive index. The scattered field is calculated as a superposition of fields emitted by point dipoles with known polarizations. Such a superposition can be calculated as a result of the interaction in the "dipole-incident radiation" system [125]. It should be noted that the residual uncertainty of modeling is up to 30 %, and taking in to account the substrate leads to poorly controlled, unstable computational processes [126, 128].

The T-matrix method describes at any point in space the scattered and internal fields induced in a scattering homogeneous medium with NPs. The method is based on the application of surface integral equations using the Green's function and expansion into infinite series of the incident, scattered, and internal fields in vector wave basis spherical functions. The T-matrix method does not describe the fields themselves in the coordinate representation, but the expansion coefficients of the incident and scattered fields in terms of some unified system of basis vector functions. These functions are determined from infinite systems of linear algebraic equations. In this method, a serious problem is the description of NPs whose shape differs from spherical [129].

The method of finite differences in the time domain (FDTD) describes the distribution of the field during the interaction of an electromagnetic wave with structures of any shape, by discretizing Maxwell's equations in differential form and subsequent uniform discretization of a region of space and time interval with the assignment of initial conditions, as it is shown in Fig. 5. Thus, the change in the electric and magnetic fields in time depends on the change in the magnetic and electric fields in space, respectively. This method refers to numerical methods for solving differential equations based on the replacement of derivatives by difference schemes. In calculations, the entire space is divided into elementary cells, and the initial conditions for all components are specified, which are decisive for field excitation [130 – 133]. In the ideal case, near one element, when the spatial grid is divided, the electromagnetic field should not undergo changes, which is equivalent to the fact that the wavelength does not experience a jump. Thus, in order to obtain adequate results, it is important that the relationship between spatial and temporal increments be maintained. The finite difference method includes the following main steps:

1. parameters are set: computational, spatial grid resolution, boundary conditions [134, 135]. When a plane wave is incident at an angle, periodic boundary conditions with a time shift are required [136];
2. inside the computational area, the constituent structures (for example, NP, environment) are created with the given values of material constants;
3. the radiation source is set (to describe the dipoles, the source is the time dependence of the current density in the Ampère equation [132]);
4. it is considered that the source excites in time a;
5. finite electromagnetic wave with wavelengths in a given range of values – depending on the boundary conditions, the incident wave can be scattered and absorbed [135, 136];
6. field values are recalculated in the frequency representation using the Fourier transform and auxiliary calculations are carried out, for example, recalculation into the optical characteristics of the nanostructure [137].

The most important advantages of this method include the following:

1. the method is adapted to spectroscopic studies, when it is necessary to calculate a large number of spectral components (since the method solves Maxwell's equations in the time domain) [114];

2. suitable for calculations where it is necessary to take in to account edge effects and screening effects [134];
3. suitable for describing anisotropic, dispersive and nonlinear media [138].

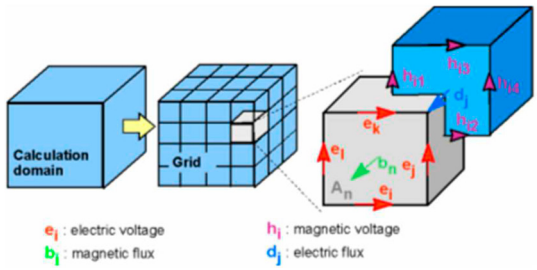

Fig. 5. Illustration of calculation on the elementary cells used in the family of finite element methods and integrals [139]

Among the most significant disadvantages of this method, it should be noted that it has serious limitations in computational efficiency when calculating the properties of extended nanostructures in the form of NP monolayers [139, 140]. So, for example, to calculate the characteristics of the electromagnetic field in the far zone (when an accurate recalculation from the components of the electromagnetic field in the near zone is impossible), the volume of the simulated space increases, which leads to a rapid increase in the volume of calculations [134, 140]. For nanostructures in the form of NP monolayers, in the case when it is necessary to increase the area of the nanostructure, it is necessary to increase the volume of the entire calculation area, which leads to a quadratic increase in the number of discretization cells [138].

A family of finite element methods and integrals. The common disadvantages of the methods described above (except for FDTD) include the complexity of describing collective interactions in the system "NP-substrate-environment ensemble" and the impossibility of describing extended nanostructures [139]. Many numerical calculation methods are still under development, improvement and modification, and for this reason there is no unified classification and hierarchy. The most widespread and generally accepted approach to the classification of methods is considered, where the finite element method is considered to be the most general [139 – 142]. In its pure form, the method of finite integrals, as well as the method of finite differences in the time domain, as a rule, are used only for broadband calculations in the time domain [143 – 145]. For narrow-band problems, where the calculation of rather complex and, especially, extended structures is required, calculations in the frequency domain based on the finite element method are used [146].

This family of methods refers to methods for solving the system of Maxwell equations in integral form. The area in which the solution of the system of Maxwell equations in integral form is sought is divided into a finite number of elements (cells). In each of the cells, some kind of approximating function is selected, which is equal to zero outside the given cell. The function values at the cell nodes are the desired ones. To find the coefficients of the approximating functions at the nodes of the cells, a system of linear algebraic equations is compiled and solved, and due to the limited number of connections for each node, the matrix of the system of linear algebraic equations is sparse. For the numerical solution of these equations, the calculation area is first determined, containing the simulated structure in the form of a set of elementary cells. In this case, the computational domain is divided into a finite number of contiguous cells, which play the role of the computational grid.

The choice of a software package for constructing a methodology for calculating the characteristics of optoacoustic transducers is associated with the need to obtain results that are repeatable and adequate to reality, while it is necessary to take in to account the main physical processes that occur during the operation of these devices.

The theoretical description of an interconnected set of problems of different physical nature requires a joint numerical solution of the fundamental interdependent equations of physics (Maxwell, Poisson) [131, 132]. Fig. 6 shows a classification of approaches for describing such an interrelated set of tasks, which can be divided into sequential [130, 131, 147] and parallel [148 – 150]. Fig. 6 also shows the main software packages in which the considered approaches can be implemented. The following modern software packages are given as examples: CST Microwave Studio, Ansys Multiphysics and Comsol Multiphysics.

In sequential methods, calculations are carried out in a chain within individual computing blocks that describe processes of various physical nature. These methods, in turn, are divided into those using unidirectional and bidirectional calculations. It is important to note that in sequential unidirectional methods, at each stage of calculations, it is possible to use different input data, as well as output calculation data from a certain computing module. At the same time, the possibility of a global organization of iterations remains [151]. In sequential bidirectional methods, iterations can be implemented at each stage of calculations, including for refining the structure between computing modules adjacent in the hierarchy. Parallel methods are a generalization of methods with bidirectional calculations: they solve systems of coupled equations, when at an intermediate stage of calculations it is not always possible to evaluate the results of calculations of a separate physical process. Also, with the parallel type of calculations, there is no possibility to conduct numerical experiments related to the hypothetical "switching off" of any physical process, which can be very useful in determining the physical mechanisms for the connection of input parameters with output ones.

Within the framework of Comsol Multiphysics, a technique with parallel iterations is implemented, when electromagnetic, thermal and mechanical properties are simultaneously calculated. Comsol Multiphysics is a software package for solving systems of partial differential equations and is often positioned as an add-on to Matlab [147], where you can set up a simulation of some physical phenomenon using a graphical interface, and

then save it as a Matlab script. Comsol Multiphysics allows you to consider physical processes that are described by equations of mathematical physics in partial derivatives, in which constants and coefficients are associated not with mathematical abstractions, but with real physical substances, processes and phenomena. The main difficulty is that it is necessary for the user to correctly formulate adequate equations that describe the problem being solved. Moreover, when using this software package, an exact specification of the boundary conditions is required. For adequate work in this package, you need to spend some time on training.

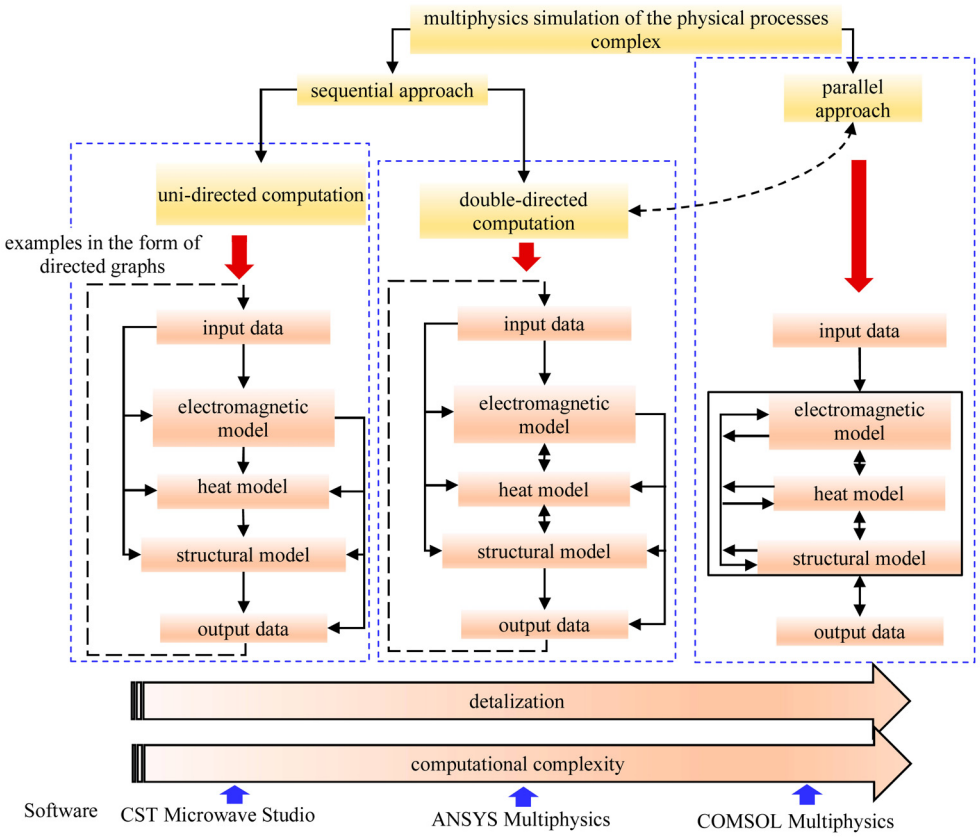

Fig. 6. Classification of approaches for describing such an interrelated set of tasks

Ansys Multiphysics generally implements sequential bidirectional methods for calculating complex physical characteristics. This software package is focused on solving low-frequency problems of electrodynamics, which is its main drawback in relation to the description of optoacoustic converters, where modeling of the interaction of optical radiation with a nanostructure is fundamentally required. Historically, the Ansys Multiphysics software package was positioned to solve problems related to electric motors, relays, and solenoids [152]. The two considered software packages are the most appropriate when, in practice, problems arise in which it is impossible not to take in to account the interaction of phenomena of different physical nature on a close time scale (temperature dependence of the dispersion of optical constants, thermal heating) [149], [152 – 155].

CST Microwave Studio implements sequential type techniques. This software package makes it possible to split the calculations into conditionally independent processes, which makes it possible to repeatedly simplify the system of related equations of physics and reduce the computational domain in space and, ultimately, obtain a solution to the problem with sufficient accuracy in an acceptable time [130]. This is especially true when there is a significant difference in the time scales of physical processes occurring in optoacoustic converters, which makes it possible to justify the use of these approximations. Historically, the CST Microwave Studio software package developed as a tool for modeling microwave structures and microwave antennas [143]. As part of this package, a whole set of verified methods of electromagnetic modeling is used (a family of finite element methods and integrals in the frequency and time domains, the method of integral equations, the method for calculating eigen electromagnetic frequencies). In the process of historical development, stationary and transient thermal calculators were added to this package, initially developed, verified and optimized for modeling electromagnetic heating, which, in fact, must be taken in to account when modeling an optoacoustic converter. In turn, the mechanical calculator as part of this software package appeared somewhat later and is positioned to simulate thermal expansion and the resulting deformations, which is necessary to implement the optoacoustic converter model.

There are some attempts to create methods for calculating the complex of characteristics of nanostructures in the form of a monolayer (and monolayers) of nanoparticles on the surface of a solid body, however, assumptions and neglects have a strong influence on the calculation results (for example, when the refractive indices of the substrate and the environment calculated as an average). Therefore, there is some discrepancy between theoretical results and experimental data. In [140], a theoretical edge experimental study of a fiber-optic ultrasonic generator was carried out, the absorbing layer in which was a nanocomposite film with spherical Au NPs 20 nm in size in a polymer matrix 10×140 μm thick, deposited on the end face of an optical fiber.

Fig. 7 shows the absorption spectrum for a monolayer of 6 spherical nanoparticles with a size of 50 nm for various distances between the centers of nanoparticles [140]. The theoretical study was carried out in the Comsol Multiphysics software package using the finite element method and a tetrahedral grid of spatial discretization. The authors of the work note that the results of calculations can only be used as estimates or initial approximations for a series of experiments. The study of the electromagnetic properties of fiber-optic optoacoustic transducers in the CST Microwave Studio software package was also carried out here by the finite element method, when hexagonal unit cells were used in the nanostructure plane, while spherical Au NPs with a size of $20 \div 50$ nm were studied at the end of the optical fibers when the distance between them varied from 75 nm to 260 nm. It was found that one layer of nanoparticles with a diameter of 50 nm makes it possible to achieve an absorption coefficient of over 50 %, and three layers of Au NPs with a size of less than 25 nm – over 90 %. With a further increase in the number of NP layers in the nanostructure, saturation occurs and the absorption coefficient does not increase. The authors note that the work is of particular interest for the further creation of experimental samples of fiber-optic optoacoustic transducers, however, to implement such a transducer even with two NP layers, when one NP layer is suspended at a certain distance above the other layer (the NP are exactly one above the other) extremely difficult. The use of nanoparticles in the form of nanocylinders with a base diameter of 50 nm and a height of 150 nm makes it possible to achieve an absorption coefficient of more than 80 %, which, however, is difficult to implement in practice, according to the authors of [140].

It should be noted that the approach to the theoretical study of the electromagnetic properties of nanostructures presented in this work has a number of disadvantages:

1. “non-physical” surges and dips are observed on the graphs (Fig. 7, dip on the black curve);
2. due to the direct calculation of the far field components, the presented approach has a low computational efficiency;
3. no comparison with experiment is given for theoretical results.

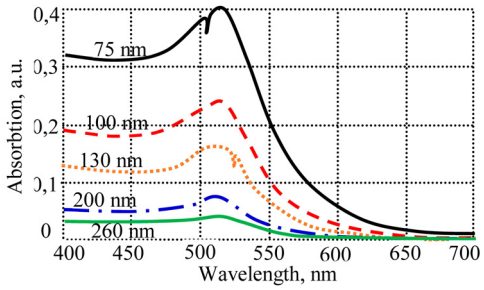

Fig. 7. Absorption spectrum for a monolayer of 6 spherical nanoparticles with a size of 50 nm for various distances between the centers of nanoparticles, carried out in the Comsol Multiphysics

The literature also cites a number of works where the results of a theoretical study are in good agreement with experimental data for other types of nanostructures [155 – 159], however, the method for calculating the complex of optoacoustic characteristics of nanostructures is not always given in full:

1. there is no study of the convergence of simulation results;
2. models of distributed structures with a high aspect ratio are not used as computational units;
3. most works do not verify theoretical results with experimental data;
4. there is no analysis of the limits of applicability of the implemented methodology.

To calculate the optical characteristics of nanostructures in the form of a monolayer of NPs on a substrate in the environment, large computing power is required, which is extremely difficult to implement in practice. However, the finite element method makes it possible to use the boundary conditions of an elementary cell, which provide modeling of a periodic structure infinite in two directions. This, based on the linearity of the interaction of optical radiation with the nanostructure, makes it possible to use the principle of superposition, since in the nanostructure in the form of a monolayer of nanoparticles on the surface of a solid body, there are a sufficient number of regions in which there is a quasi-periodic arrangement of nanoparticles. Moreover, in nanostructures in the form of a monolayer of nanoparticles on the surface of a solid body, collective interactions take place in the system “ensemble of nanoparticles-substrate-environment”, which allows us to speak about the formation of a “collective” electromagnetic field [160, 161]. The superposition of the responses of an ensemble of such regions forms the response of the entire nanostructure in practice. Fig. 8 shows experimental absorption spectrum for a periodic and non-periodic nanostructures in the form of a cylindrical NP with a diameter of 150 nm and a period 550 nm.

It is important to note that a number of authors studied the influence of the periodicity of the arrangement of NPs in a monolayer on the surface of a solid body on the spectral parameters of the absorption band [38, 162]. Fig. 9*a*, *b* shows micrographs of scanning electron microscopy of an experimental sample of a periodic and

non-periodic (average distance between NP centers 699 nm and the number of iterations of random displacements N = 10) nanostructure in the form of a monolayer of Au NPs.

To quantitatively describe the degree of non-periodicity of NPs on a substrate in a nanostructure, the following method was used [38]:

1. a grid with square cells was numerically generated;
2. based on the generated grid, a photomask was formed with periodically located NPs on the substrate, where the NPs were located at the nodes of the grid, and a periodic nanostructure was fabricated from it. Fig. 9*a* shows a scanning electron microscopy micrograph of an experimental sample of a periodic (500 nm period) nanostructure in the form of a monolayer of Au NPs on a substrate;
3. the positions of the nodes in the generated grid were shifted randomly, and the statistical properties of the shifts along each of the coordinates obeyed the Gaussian distribution;
4. random shifts of nodes are carried out iteratively an integer number N times;
5. based on the generated spatial distribution matrix, a photomask was formed with randomly located nanoparticles on a substrate, and a nanostructure was fabricated on its basis.

Fig. 8 shows the experimental absorption spectrum for a periodic (the number of iterations of random displacements N = 0) and non-periodic (the number of iterations of random displacements N = 5, 10) nanostructures in the form of a cylindrical NP with a diameter of 150 nm and a period (the average distance between LF) 550 nm [38].

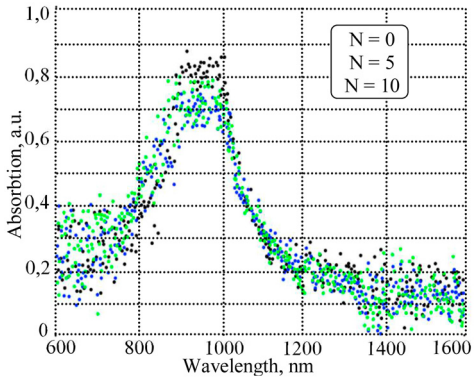

Fig. 8. Experimental absorption spectrum for a periodic (the number of iterations of random displacements N = 0) and non-periodic (the number of iterations of random displacements N = 5, 10) nanostructures in the form of a cylindrical NP with a diameter of 150 nm and a period (the average distance between LF) 550 nm [38]

It can be seen that, in a periodic structure with a monolayer of Au NPs on a substrate, a somewhat narrower SPR is observed with an intensity greater than the intensity of that spectrum for a nonperiodic nanostructure.

The authors of [9] note that the position of the SPR peak weakly depends on the degree of non-periodicity of the arrangement of NPs in the composition of the nanostructure, however, in general, the main spectral parameters, such as the width of the SPR peak, the absorption value in the SPR peak, change by no more than 10 – 20 %. If we recalculate the given sizes and periods of NP location to the substrate filling density parameter adopted in this work, then the conclusion made by the authors is valid for substrate filling densities up to 50 – 60 %.

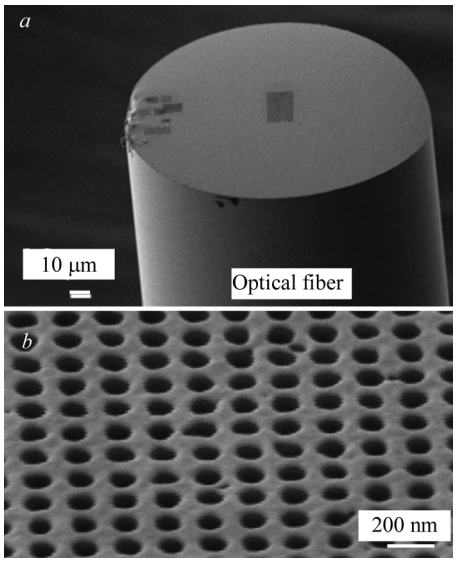

Fig. 9. Example of periodic absorbing nanostrusture

5. Multiphysics simulation of optoacoustic transducers based on forced acoustic oscillations

In the case of fiber-optic optoacoustic transducer, laser driver provides generation of intensity-modulated laser signal, which is absorbed at optical fiber edge. Absorber (monolayer of NPs) is heated and cooled, leading to the local pressure modulation, which, in turn, results in generation of ultrasound acoustic waves.

Whole complex of physical phenomena leads to the excitation of sound in the medium: elastic stress at the particle-medium interface, elastic stress at the particle-substrate interface, and, to a lesser extent, the substrate medium. So, at least, the following simulation sequence should be performed in order to find out the relationship between the modulated optical power and the output acoustic characteristics of the optoacoustic transducer:

1. Calculate the optical absorption coefficient in the surface nanostructure at the optical fiber edge for an emission wavelength of commercially available laser (electromagnetic simulation was studied in details by authors in the [160 – 162]);
2. Calculate available heat emission power for the some laser type and for each set of nanostructure microscopic parameters (available heat emission power is equal to the product of absorbtion coefficient and laser power [162]);
3. Simulate steady-state temperature distribution within the nanostructure for stationary value of heat emission power in order to check the possibility of physical implementation of such structures with long-term op-

eration without overheating (steady-state thermal modelling);

4. For time-varying heat emission power, simulate a time-varying temperature distribution in the nanostructure and its surrounding. During this stage, durations of heat transfer transients are determined by means of analysis of the set of instantaneous temperature and heat flux 3D distributions;
5. Simulate mechanical displacements of the nanostructure components and resulting time-varying pressure (mechanical modeling).

As it mentioned previously, when modeling thermal expansion within the complex of physical problems, nanoparticles under study are not considered as free. The thermal and elastic properties the spatially fixed substrate of optical fiber edge as well as the environment surrounding are taken in to account. Moreover, when modeling and solving structural analysis problems, appropriate boundary conditions are applied [83, 112].

Thermophysical simulation of optoacoustic transducers (2 – 4) is a multi-step process. Firstly, it is necessary to define the limitations numerical model of the nanostructure. Then, set the boundary conditions should be chosen. Optoacoustic transducer consisting of monolayer of monodisperse metal NPs on a substrate (optical fiber edge) has been simulted with the CST Microwave Studio SE [160, 163]. Surface nanostructure simulation is realized using the unit cell boundary conditions (translation is carried out in two dimensions to infinity). The unit cell of the nanostructure consists of four contiguous parallelepipeds, two of which consist of a substrate material, and the other two contain a surrounding material. NPs are placed at the interface between substrate and surrounding (with the base touching the substrate). The usage of additional parallelepipeds of the same material is associated with better convergence and limited processing power [161], remaining two layers are semi-infinite due to absorbing boundary conditions [165 – 168]. Nevertheless, random spatial distribution of NPs on the solid substrate results in slightly wider SPR-peak with decreased intensity. It is noted [162], that the main spectral parameters (e.g., SPR-peak position, absorbtion coefficient at the SPR-peak and its width) are changed no more then on the amount of 10 – 20% [162].

After, it is necessary to calculate steady-state as well as time-varying temperature distribution in the nanostructure and its surrounding. Fig. 10*a* shows layout of thermophysical simulation of surface nanostructures for optoacoustic fiber-optic transducers. As it was shown previously, surface nanostructure is characterized by very high aspect ratio [160]. Therefore, uniform temperature distribution boundaries can be used at some distance from the monolayer of NPs. In the case of heat transfer problems, such approximation can be used in planes, which are parallel to optical fiber edge and are situated at the distance exceeding 5 – 10 NP diameters. This allows using isothermal boundary conditions, which is physically equivalent to the presence of an infinite heat reservoir.

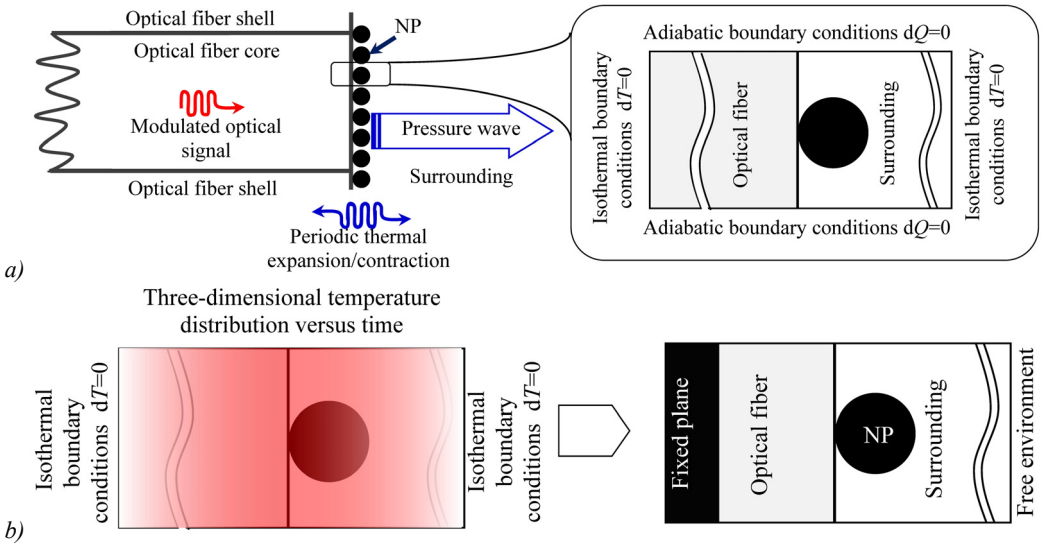

Fig. 10. Layout of thermophysical (a) and mechanical (b) simulation of surface nanostructures for optoacoustic fiber-optic transducers

Actually, the volume of the nanostructure at the optical fiber edge is negligible (for example, at least, several tens of centimeters of optical fiber correspond to the relative volume fraction of the nanostructure $10^{-12} – 10^{-13}$). Previously, the authors found that an ordered electromagnetic field distribution is formed near the mode spot center at the optical fiber edge [31, 40 – 42, 46]. For this reason, it can be assumed that there is no heat transfer along the plane, which is parallel to the optical fiber edge. At least, there is no significant heat transfer between the NPs. Therefore, it is possible to apply adiabatic boundary conditions in use in the plane between NPs, which is orthogonal to optical fiber edge.

Fig. 10*b* shows layout of mechanical simulation of surface nanostructures for optoacoustic fiber-optic transducers. Mechanical parameters of the media (Young's

modulus, Poisson's ratio, coefficient of thermal expansion) are set and, a plane parallel to the optical fiber edge is fixed for implementation a mechanical model of a nanostructure as part of an optoacoustic transducer After, the 3D time-varying temperature distribution is taken into account. As a result of mechanical modeling, the strain tensor is calculated, as well as the tensor of mechanical stresses. Pressure is the hydrostatic stress, which is the average of the diagonal elements of the tensor of mechanical stresses.

Such approach allows to establish relationship between nanostructure microscopic parameters, modulated optical power and the output acoustic characteristics of the optoacoustic transducer. For example, it is shown that the applicability of nanostructures in air as optoacoustic transducer is not limited by thermal destruction of the nanostructure, while the thermophysical limitations for nanostructures in water are explained by boiling.

Comprehensive study of nanostructures with a help of such approach made it possible to establish that the type of nanostructure for optoacoustic transducer, should be selected based on a compromise between the performance requirements, and realization simplicity.

6. Example of experimental study of optoacoustic device

The following experimental procedure illustrates example of optoacoustic response measurement [170]. Silver NPs monolayer has been deposited on the optical fiber edge using pulsed laser deposition method [169].

Fig. 12 shows photo of the setup for investigation of a fiber-optic optoacoustic transducer with nanoparticles monolayer deposited on the optical fiber edge within liquid surrounding [168]. TiePie HS5 (oscilloscope with arbitrary waveform generator) generates probe pulses with a period of 10 ms, a duration of 50 ns, fronts less than 12 ns, and an amplitude of 12 V from a digital arbitrary signal generator of arbitrary. Probe electrical pulses are guided towards to fiber-coupled laser Laserscom LDI-450-FP-30 by means of coaxial cable. The optical signal parameters within the optical fiber are measured by means of 01 %:99 % fiber-optic coupler, Vishay BPF34 photodiode and control channel of TiePie HS5. The peak optical power at 450 nm is estimated as high as 40 mW. The most part of the intensity-modulated optical signal (99 %) is connected via a Seikoh Giken SNA-1 fiber-optic adaptor the SMF-28e optical fiber with deposited surface nanostructures. The prototype of optoacoustic transducer, in turn, is positioned by Standa 7T38 XYZ system. An acoustic signal is detected by a SoarPiezo 10×0.20mm-PZT5 narrowband hydrophone. Spherical NPs are used, the analysis of series of binarized photos allows to conclude that NPs are characterized by gamma-distribution with average size of 35 nm, RMS size variation of 12 nm and surface occupation density of 3.8 %.

The hydrophone signal is detected by the measurement channel of high dynamic range oscilloscope TiePie HS5 (a maximum relative uncertainty of signal level measurement is 0.25 %). The operation frequency range of the proposed setup exceeds 40 MHz.

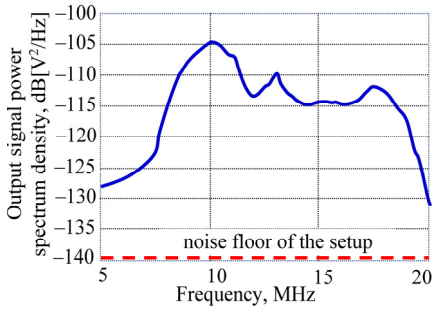

Fig. 11. Power spectrum density of the output signal for the prototype of optoacoustic transducer with monolayer of silver nanoparticles within water surrounding [170]

Fig. 11 shows measured power spectrum density of the output signal for the prototype of optoacoustic transducer with monolayer of silver nanoparticles within water surrounding. The power spectral density of the electrical signal at the hydrophone output [V^2/Hz] is directly proportional to the energy [J] and is determined by the acoustic energy [Pa^2]. One can see that the optoacoustic response is observed in the frequency range of 10 – 18 MHz and its level is more than 12 dB higher than setup noise floor.

The optoacoustic response is experimentally observed in the frequency range of 10 – 18 MHz for surface nanostructure with average size of nanoparticles of 35 nm, RMS size variation of 12 nm and surface occupation density of 3.8 % [170]. This is in a good agreement with theoretical results.

Conclusion

Optoacoustic transducers and receivers are used in very wide range of applications from engineering flaw detection and medical diagnostics to optoacoustic communication. The choice of optoacoustic devices as a physical diagnostic tool is of particular importance, which allows to identify the exact coordinates of a particular defect, violation of the structure or composition of a substance, including critical ones. It is shown that miniaturization of the ultra-sound source is topical for studying small optoacoustic structures.

One can see that optoacoustic ultrasonic receivers allows all-optical detection of acoustic waves for very different situations under study. They allow to receive acoustic signals with frequencies up to 140 MHz with the effective sensor size less than 100 μm. The analysis of the set of papers shows that this topic is rather developed. But, it is not in the area of scientific, but technical problems.

From the other hand, optoacoustic transducers are less studied scientific problem. The world scientific community has already accumulated enough knowledge about the physical processes underlying optoacoustic conversion. The main problem currently standing between us and really high-performance devices with wide operating frequency bands is that the energy conversion process has

many parameters, which significantly complicates its optimization. The combination of a metal and a polymer in the hybrid material of the active medium of an optoacoustic transducer to combine their "useful" properties (the ability to absorb laser radiation and high thermal diffusivity for a metal and a high coefficient of linear thermal expansion for a polymer) always leads to the appearance in the final material of "harmful" properties of the components.

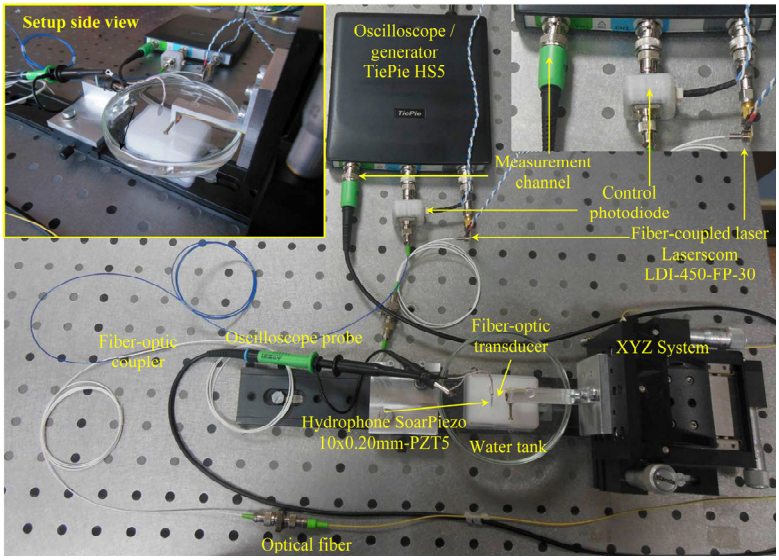

Fig. 12. Photo of the setup for investigation of a optoacoustic transducer with nanoparticles monolayer deposited on the optical fiber edge within liquid surrounding [170]

For high energy efficiency of an optoacoustic ultrasonic transducer, it is necessary to find the optimal combination of many system parameters, in particular, the optical and thermophysical properties of its constituent materials. Since the process is multiparametric, it would be convenient to apply modern methods of computer algorithms, such as genetic algorithms and machine learning, to optimize the structure and select the materials included in it. So, the simulation methods of the optoacoustic transducers are of extreme importance. Comprehensive study of nanostructures with a help of multiphysics approach made it possible to establish that the design for acoustic transducer, should be selected based on a compromise between the performance requirements, and realization simplicity. Up to the moment, the optoacoustic response has been experimentally observed in a good agreement with theoretical results.

Acknowledgments

The work has been supported by the Russian Science Foundation 21-12-00304.

References

[1] Czichos H. Technical diagnostics: principles, methods, and applications. NCSLI Measure 2014; 9(2): 32-40.
[2] Worden K, et al. The fundamental axioms of structural health monitoring. Philos Trans Royal Soc A 2007; 463(2082): 1639-1664.
[3] Sposito G, et al. A review of non-destructive techniques for the detection of creep damage in power plant steels. NDT E Int 2010; 43(7): 555-567.
[4] Hu C, Yu Z, Wang A. An all fiber-optic multi-parameter structure health monitoring system. Opt Express 2016; 24(18): 20287-20296.
[5] Li W, Lan Z, Hu N, Deng M. Modeling and simulation of backward combined harmonic generation induced by one-way mixing of longitudinal ultrasonic guided waves in a circular pipe. Ultrasonics 2021; 113: 106356. DOI: 10.1016/j.ultras.2021.106356.
[6] Kim S, Choi C, Cha Y, et al. The efficacy of convenient cleaning methods applicable for customized abutments: an in vitro study. BMC Oral Health 2021; 21: 78. DOI: 10.1186/s12903-021-01436-z.
[7] Biagi E, Margheri F, Menichelli D. Efficient laser-ultrasound generation by using heavily absorbing films as targets. IEEE Trans Ultrason Ferroelectr Freq Control 2001; 48(6): 1669-1679.
[8] Yang H, et al. Characterization of a broadband all-optical ultrasound transducer – from optical and acoustical properties to imaging. Appl Phys Lett 2007; 91: 073507.
[9] Yang T. Surface plasmon cavities on optical fiber end-facets for biomolecule and ultrasound detection. Opt Laser Technol 2018; 101: 468-478.
[10] Lyamshev LM. Optoacoustic sources of sound. Sov Phys Usp 1981; 24: 977-995.
[11] Naugolnykh KA, Ostrovsky LA. Nonlinear wave processes in acoustics. Cambridge: Cambridge University Press; 1998.
[12] Akhmanov SA, Rudenko VZh. Parametric laser emitter of ultrasound [In Russian]. Jurnal Tehnicheskoi Fiziki 1975; 1(15: 725-728.
[13] Martellucci S. Analytical laser spectroscopy. Springer Science & Business Media; 2012.
[14] Stewart RB, Diebold GJ. Radiation - induced thermal noise in optoacoustic detection cells. J Appl Phys 1984; 56: 1992-1996. DOI: 10.1063/1.334233.
[15] Werner JPF, Mishra K, Huang Y, Vetschera P, Glasl S, Chmyrov A, Richter K, Ntziachristos V, Stiel AC. Structure-based mutagenesis of phycobiliprotein smURFP for optoacoustic imaging. ACS Chem Biol 2019; 14: 1896-1903.
[16] Yoshida S, Adhikari S, Gomi K, Shrestha R, Huggett D, Miyasaka C, Park I. Opto-acoustic technique to evaluate

adhesion strength of thin-film systems. AIP Advances 2012; 2: 022126. DOI: 10.1063/1.4719698.
[17] Kostli KP, Frauchiger D, Niederhauser JJ, Paltauf G, Weber HP, Frenz M. Optoacoustic imaging using a three-dimensional reconstruction algorithm. IEEE J Sel Top Quantum Electron 2001; 7(6): 918-923. DOI: 10.1109/2944.983294.
[18] Wu N, et al. Fiber optic ultrasound transmitters and their applications. Measurement 2016; 79: 164-171.
[19] Nishijima Y, Rosa L, Juodkazis S. Surface plasmon resonances in periodic and random patterns of gold nano-disks for broadband light harvesting. Opt Express 2012; 20(10): 11466-11477.
[20] Tian Y, et al. Numerical simulation of gold nanostructure absorption efficiency for fiber-optic optoacoustic generation. Prog Electromagn Res Lett 2013; 42: 209-223.
[21] Gaponenko SV. Introduction to nanophotonics. Cambridge: Cambridge University Press; 2010.
[22] Baranov AV, et al. Technique of physical experiment in systems with reduced dimension [In Russian]. Saint-Petersburg: "SPbGU ITMO" Publisher; 2009.
[23] Hutter E, Fendler JH. Exploitation of localized surface plasmon resonance. Adv Mater 2006; 16: 1685-1706.
[24] Lakowicz JR, et al. Plasmon-controlled fluorescence: a new detection technology. Proc SPIE 2006; 6099: 609909.
[25] Noguez C. Surface plasmons on metal nanoparticles: the influence of shape and physical environment. J Phys Chem C 2007; 111: 3806-3819.
[26] Sekhon JS, Verma SS. Refractive index sensitivity analysis of Ag, Au, and Cu nanoparticles. Plasmonics 2011; 6: 311-317.
[27] Hutter TS, Elliott R, Mahajan S. Interaction of metallic nanoparticles with dielectric substrates: effect of optical constants. Nanotechnology 2013; 24: 035201.
[28] Rivero PJ, Goicoechea J, Arregui FJ. Localized surface plasmon resonance for optical fiber-sensing applications. In Book: Barbillon G, ed. Nanoplasmonics – Fundamentals and applications. IntechOpen; 2017: 399-429.
[29] Singh CD, Shibata Y, Ogita M. A theoretical study of tapered, porous clad optical fibers for detection of gases. Sens Actuators B Chem 2003; 92: 44-48.
[30] Zhou J, et al. Water temperature measurement using a novel fiber optic ultrasound transducer system. 2015 IEEE Int Conf on Information and Automation 2015: 2316-2319.
[31] Yang L. Miniaturized fiber optic ultrasound sensor with multiplexing for photoacoustic imaging. Photoacoustics 2022; 28: 100421.
[32] Bi S. Ultrasonic transmission from fiber optic generators on steel plate. Proc SPIE 2016; 9804: 98040Q.
[33] Du C. All-optical optoacoustic sensors for steel rebar corrosion monitoring. Sensors 2018; 18(5): 1353-1365.
[34] Zhou J, et al. High temperature monitoring using a novel fiber optic ultrasonic sensing system. Proc SPIE 2018; 10639: 1063910.
[35] Jensen JA. Medical ultrasound imaging. Prog Biophys Mol Biol 2007; 93: 153-165.
[36] Nelson TR, Pretorius TH. Three-dimensional ultrasound imaging. Ultrasound Med Biol 1998; 24(9): 1243-1270.
[37] von Haxthausen F, Böttger S, Wulff D, et al. Medical robotics for ultrasound imaging: Current systems and future trends. Curr Robot Rep 2021; 2: 55-71.
[38] Yu Y, Safari A, Niu X, Drinkwater B, Horoshenkov KV. Acoustic and ultrasonic techniques for defect detection and condition monitoring in water and sewerage pipes: A review. Appl Acoust 2021; 183: 108282.
[39] Bombarda D, Vitetta GM, Ferrante G. Rail diagnostics based on ultrasonic guided waves: An overview. Appl Sci 2021; 11(3): 1071.
[40] Liu S, Sun Y, Jiang X, et al. A review of wire rope detection methods, sensors and signal processing techniques. J Nondestr Eval 2020; 39: 85.
[41] Mangalgiri PD. Corrosion issues in structural health monitoring of aircraft. ISSS J Micro Smart Syst 2019; 8: 49-78.
[42] Stras B, Conrad C, Walter B. Production integrated non-destructive testing of composite materials and material compounds – An overview. IOP Conference Series: Materials Science and Engineering 2017; 181: 12017.
[43] Vavilov VP. Thermal nondestructive testing of materials and products: a review. Russ J Nondestruct Test 2017; 53: 707-730.
[44] Toh N, Akagi T, Kasahara S, et al. Evolution of echocardiography in adult congenital heart disease: from pulsed-wave Doppler to fusion imaging. J Echocardiogr 2021; 19: 205-211.
[45] Takaya Y, Ito H. New horizon of fusion imaging using echocardiography: its progress in the diagnosis and treatment of cardiovascular disease. J Echocardiogr 2020; 18: 9-15.
[46] Meola M, Ibeas J, Lasalle G, Petrucci I. Basics for performing a high-quality color Doppler sonography of the vascular access. J Vasc Access 2021; 22(1): 18-31.
[47] Martin KH, Dayton PA. Current status and prospects for microbubbles in ultrasound theranostics. WIREs Nanomed Nanobiotechnol 2017; 5: 329-345.
[48] Dasgupta A, Liu M, Ojha T, Storm G, Kiessling F, Lammers T. Ultrasound-mediated drug delivery to the brain: principles, progress and prospects. Drug Discovery Today: Technologies 2016; 20: 41-48.
[49] Duric N, Littrup P, Poulo L, Babkin A, Pevzner R, Holsapple E, Rama O, Glide C. Detection of breast cancer with ultrasound tomography: First results with the Computed Ultrasound Risk Evaluation (CURE) prototype. Med Phys 2007; 34: 773-785.
[50] Mahmud M, Islam MS, Ahmed A, Younis M, Choa F-S. Cross-medium optoacoustic communications: challenges, and state of the art. Sensors 2022; 22(11): 4224. DOI: 10.3390/s22114224.
[51] Ji Z, Fu Y, Li J, Zhao Z, Mai W. Optoacoustic communication from the air to underwater based on low-cost passive relays. in IEEE Commun Mag 2021; 59(1): 140-143. DOI: 10.1109/MCOM.001.2000607.
[52] Sullenberger RM, Kaushik S, Wynn CM. Optoacoustic communications: delivering audible signals via absorption of light by atmospheric H2O. Opt Lett 2019; 44: 622-625.
[53] Schmid, T. Optoacoustic spectroscopy for process analysis. Anal Bioanal Chem 2006; 384: 1071-1086. DOI: 10.1007/s00216-005-3281-6.
[54] Holthoff EL, Heaps DA, Pellegrino PM. Development of a MEMS-scale optoacoustic chemical sensor using a quantum cascade laser. IEEE Sensors J 2010; 10(3): 572-577. DOI: 10.1109/JSEN.2009.2038665.
[55] Mothé G, Castro M, Sthel M, Lima G, Brasil L, Campos L, Rocha A, Vargas H. Detection of greenhouse gas precursors from diesel engines using electrochemical and optoacoustic sensors. Sensors 2010; 10(11): 9726-9741. DOI: 10.3390/s101109726.
[56] Elia A, Di Franco C, Lugarà PM, Scamarcio G. Optoacoustic spectroscopy with quantum cascade lasers for trace gas detection. Sensors 2006; 6(10): 1411-1419. DOI: 10.3390/s6101411.

[57] Zharov VP, Galanzha EI MD, Shashkov EV, Kim J-W, Khlebtsov NG, Tuchin VV. Optoacoustic flow cytometry: principle and application for real-time detection of circulating single nanoparticles, pathogens, and contrast dyes in vivo. J Biomed Opt 2007; 12(5): 051503.
[58] Johnson S, Proctor M, Bluth E, Smetherman D, Baumgarten K, Troxclair L, Bienvenu M. Evaluation of a hydrogen peroxide-based system for high-level disinfection of vaginal ultrasound probes. J Ultrasound Med 2013; 32: 1799-1804. DOI: 10.7863/ultra.32.10.1799.
[59] Lazarotto JS, Júnior EPM, Medeiros RC, et al. Sanitary sewage disinfection with ultraviolet radiation and ultrasound. Int J Environ Sci Technol 2021; 19, 11531-11538. DOI: 10.1007/s13762-021-03764-7.
[60] Khaire RA, Thorat BN, Gogate PR. Applications of ultrasound for food preservation and disinfection: A critical review. J Food Process Preserv 2021; 46(10): e16091. DOI: 10.1111/jfpp.16091.
[61] Jatzwauk L, Schöne H, Pietsch H. How to improve instrument disinfection by ultrasound. J Hosp Infect 2001; 48(A): S80-S83. DOI: 10.1016/S0195-6701(01)90019-2.
[62] Winkler AM, Maslov K, Wang LV. Noise-equivalent sensitivity of photoacoustics. J Biomed Opt 2013; 18(9): 97003.
[63] Kim KH, et al. Air-coupled ultrasound detection using capillary-based optical ring resonators. Sci Rep 2017; 7: 109.
[64] Wissmeyer G, et al. Looking at sound: optoacoustics with all-optical ultrasound detection. Light Sci Appl 2018; 7: 53.
[65] Liang Y. Fiber-laser-based ultrasound sensor for photoacoustic imaging. Sci Rep 2017; 7: 40849.
[66] Zhou J. High temperature monitoring using a novel fiber optic ultrasonic sensing system. Proc SPIE 2018; 10639: 1063910.
[67] Dong B, Sun C, Zhang H. Optical detection of ultrasound in photoacoustic imaging. IEEE Trans Biomed Eng 2017; 64(1): 4-15.
[68] Zhou QF, et al. Piezoelectric films for high frequency ultrasonic transducers in biomedical applications. Progr. in materials sci. – 2011 – Vol. 56 –P. 139–174.
[69] Li X, et al. 80-MHz intravascular ultrasound transducer using PMN-PT free-standing film. IEEE Trans Ultrason Ferroelectr Freq Control 2011; 58: 2281-2288.
[70] Niederhauser JJ, et al. Transparent ITO coated PVDF transducer for optoacoustic depth profiling. Opt Commun 2005; 253: 401-406.
[71] Rousseau G, et al. Non-contact biomedical photoacoustic and ultrasound imaging. J Biomed Opt 2012; 17: 61217.
[72] Nuster R, et al. Downstream Fabry-Perot interferometer for acoustic wave monitoring in photoacoustic tomography. Opt Lett 2011; 36: 981-983.
[73] Beard PC, et al. Transduction mechanisms of the Fabry-Perot polymer film sensing concept for wideband ultrasound detection. IEEE Trans Ultrason Ferroelectr Freq Control 1999; 46: 1575-1582.
[74] Beard PC, Mills TN. An optical detection system for biomedical photoacoustic imaging. Proc SPIE 2000; 3916: 100-109.
[75] Grun H, et al. Polymer fiber detectors for photoacoustic imaging. Proc SPIE 2010; 7564: 75640M.
[76] Rosenthal A, et al. Wideband optical sensing using pulse interferometry. Opt Express 2012; 20: 19016-19029.
[77] Sheaff C, Ashkenazi S. A fiber optic optoacoustic ultrasound sensor for photoacoustic endoscopy. Proc Ultrasonics Symp 2010: 2135-2138.
[78] Govindan, V. Bragg waveguide ultrasound detectors / V. Govindan, S. Ashkenazi // IEEE Trans. on ultrason. ferroelectr. and freq. contr. – 2012 – Vol. 59 – P. 2304–2311.
[79] Chao CY, et al. High-frequency ultrasound sensors using polymer microring resonators. IEEE Trans Ultrason Ferroelectr Freq Control 2007; 54: 957-965.
[80] Ling T, et al. Fabrication and characterization of high Q polymer micro-ring resonator and its application as a sensitive ultrasonic detector. Opt Express 2011; 19: 861-869.
[81] Scruby CB, Drain LE. Laser ultrasonics techniques and applications. New York: CRC Press; 1990.
[82] Gusev V, Karabutov A. Laser optoacoustics. NASA STI/Recon Technical Report A 1991; 93: 16842.
[83] Girshova EI, Mikitchuk AP, Belonovski AV, Morozov KM, Ivanov KA, Pozina G, Kozadaev KV, Egorov AYu, Kaliteevski MA. Proposal for a photoacoustic ultrasonic generator based on Tamm plasmon structures. Opt Express 2020; 28: 26161-26169. DOI: 10.1364/OE.400639.
[84] Ling T, et al. Fabrication and characterization of high Q polymer micro-ring resonator and its application as a sensitive ultrasonic detector. Opt Express 2011; 19: 861-869.
[85] Zhigarkov VS, Yusupov VI. Impulse pressure in laser printing with gel microdroplets. Opt Laser Technol 2021; 137: 106806. DOI: 10.1016/j.optlastec.2020.106806.
[86] Kozhushko VV, Hess P. Nondestructive evaluation of microcracks by laser-induced focused ultrasound. Appl Phys Lett 2007; 91: 224107.
[87] Baac HW, et al. Photoacoustic concave transmitter for generating high frequency focused ultrasound. Proc SPIE 2010; 7564: 116-121.
[88] Passler K, et al. Laser-generation of ultrasonic X-waves using axicon transducers. Appl Phys Lett 2009; 94: 64108.
[89] Baac HW, et al. Carbon-nanotube optoacoustic lens for focused ultrasound generation and high-precision targeted therapy. Sci Rep 2012; 2: 989-997.
[90] Chan W, Hies T, Ohl CD. Laser-generated focused ultrasound for arbitrary waveforms. Appl Phys Lett 2016; 109: 174102.
[91] Hou Y, et al. Improvements in optical generation of high-frequency ultrasound. IEEE Trans Ultrason Ferroelectr Freq Control 2007; 54: 682-686.
[92] Lee SH. Reduced graphene oxide coated thin aluminum film as an optoacoustic transmitter for high pressure and high frequency ultrasound generation. Appl Phys Lett 2012; 101: 241909.
[93] Hou Y, et al. Optical generation of high frequency ultrasound using two-dimensional gold nanostructure. Appl Phys Lett 2006; 89: 93901.
[94] Zou X, et. al. Polydimethylsiloxane thin film characterization using all-optical photoacoustic mechanism. Appl Opt 2013; 52(25): 6239-6244.
[95] Hsieh BY, et al. A laser ultrasound transducer using carbon nanofibers–polydimethylsiloxane composite thin film. Appl Phys Lett 2015; 106: 21902.
[96] Chang WY, et al. Candle soot nanoparticles-polydimethylsiloxane composites for laser ultrasound transducers. Appl Phys Lett 2015; 107: 161903.
[97] Biagi E, et al. Fiber optic broadband ultrasonic probe. 2009 IEEE Int Ultrasonics Symp 2009: 363-366.
[98] Colchester RJ, et al. Laser-generated ultrasound with optical fibres using functionalised carbon nanotube composite coatings. Appl Phys Lett 2014; 104: 173502.
[99] Colchester RJ, et al. Broadband miniature optical ultrasound probe for high resolution vascular tissue imaging. Biomed Opt Express 2015; 6: 1502-1511.

[100] Wu N, et. al. Fiber optics photoacoustic generation using gold nanoparticles as target. Proc SPIE 2011; 7981: 798118.
[101] Wu N, et al. Study of the compact fiber optic photoacoustic ultrasonic transducer. Proc SPIE 2012; 8345: 83453Z.
[102] Tian Y. Numerical simulation of fiber-optic photoacoustic generator using nanocomposite material. J Comput Acoust 2013; 21: 1350002.
[103] Tian Y, et. al. Fiber-optic ultrasound generator using periodic gold nanopores fabricated by a focused ion beam. Opt Eng 2013; 52(6): 65005.
[104] Wu N, et al. Fiber optic photoacoustic ultrasound generator based on gold nanocomposite. Proc SPIE 2013; 8694: 86940Q.
[105] Zou X, et al. Broadband miniature fiber optic ultrasound generator. Opt Express 2014; 22(15): 18119-18127.
[106] Lee J, Zaigham SB, Paeng D-G. Shock wave characterization using different diameters of an optoacoustic carbon nanotube composite transducer. Appl Sci 2022; 12: 7300. DOI: 10.3390/app12147300.
[107] Shi L, Jiang Y, Fernandez FR, et al. Non-genetic photoacoustic stimulation of single neurons by a tapered fiber optoacoustic emitter. Light Sci Appl 2021; 10: 143. DOI: 10.1038/s41377-021-00580-z.
[108] Jiang Y. High precision optoacoustic neural modulation. Doctoral dissertation. Boston University; 2021.
[109] Du X, Li J, Niu G, et al. Lead halide perovskite for efficient optoacoustic conversion and application toward high-resolution ultrasound imaging. Nat Commun 2021; 12: 3348. DOI: 10.1038/s41467-021-23788-4.
[110] Hu X, Ma Y, Wan Q, Ying K-N, Dai L-N, Hu Z, Chen F, Guan F, Ni C, Guo LB. Laser ultrasonic improvement and its application in defect detection based on the composite coating method. Appl Opt 2022; 61: 4145-4152.
[111] Girshova EI, Mikitchuk EP, Belonovskii AV, et al. An optoacoustic ultrasound generator based on a tamm plasmon and organic active layer structure. Tech Phys Lett 2021; 47: 336-340. DOI: 10.1134/S1063785021040076.
[112] Liu S, Kim H, Huang W, Chang W-Y, Jiang X, Ryu JE. Multiscale and multiphysics FEA simulation and materials optimization for laser ultrasound transducers. Mater Today Commun 2022; 31: 10359. DOI: 10.1016/j.mtcomm.2022.103599.
[113] Girshova EI, Ogurtcov AV, Belonovski AV, Morozov KM, Kaliteevski MA. Genetic algorithm for optimizing Bragg and hybrid metal-dielectric reflectors. Computer Optics 2022; 46(4): 561-566. DOI: 10.18287/2412-6179-CO-1128.
[114] Weiland T. RF & microwave simulators – from component to system design. 33rd European Microwave Conf Proc 2003; 2: 591-596.
[115] Moreno F, Saiz JM, Gonzalez F. Light scattering by particles on substrates. theory and experiments–nanostructure science and technology. New York: Springer; 2007: 305-340.
[116] Saleh BEA, Teich MC. Fundamentals of Photonics. John Wiley & Sons Inc; 1991.
[117] Ghaforyan H, Ebrahimzadeh M, Bilankohi SM. Study of the optical properties of nanoparticles using Mie theory. World Appl Program 2015; 5(4): 79-82.
[118] Fabelinskii IL. Molecular scattering of light. New York: Plenum Press; 1968.
[119] Lindell IV, et al. Exact-image theory formulation. J Opt Soc Am A 1991; 8: 472-476.
[120] Dmitriev A. Nanoplasmonic sensors. New York: Springer; 2012.
[121] Sonnichsen C, et al. Drastic reduction of plasmon damping in gold nanorods. Phys Rev Lett 2002; 88(4): 077402.
[122] Petryayeva E, Krull UJ. Localized surface plasmon resonance: nanostructures, bioassays and biosensing–A review. Anal Chim Acta 2011; 706: 8-24.
[123] Willets KA, Van Duyne RP. Localized surface plasmon resonance spectroscopy and sensing. Annu Rev Phys Chem 2007; 58: 267-297.
[124] Klimov V. Nanoplasmonics. New York: Jenny Stanford Publishing; 2014.
[125] Novotny L, Hecht B. Principles of nanooptics. New York: Cambridge University Press; 2006.
[126] Malinsky MD, et al. Nanosphere lithography: effect of substrate on the localized surface Plasmon resonance spectrum of silver nanoparticles. J Phys Chem 2001; 105(12): 2343-2350.
[127] Yurkin MA, Huntemann M. Rigorous and fast discrete dipole approximation for particles near a plane interface. J Phys Chem 2015; 119(52): 29088-29094.
[128] Amendola V, Bakr OM, Stellacci F. A study of the surface plasmon resonance of silver nanoparticles by the discrete dipole approximation method: effect of shape, size, structure, and assembly. Plasmonics 2010; 5: 85-97.
[129] Mishchenko MI, Travis LD, Mackowski DW. T-matrix computations of light scattering by nonspherical particles: A review. J Quant Spectrosc Radiat Transfer 1996; 55: 535-575.
[130] Kurushin AA, Plasticov AN. Designing microwave devices in the environment CST Microwave Studio [In Russian]. Moscow: MPEI Publishing House, 2010: 47-73.
[131] Borovkov AI, et al. Computer engineering [In Russian]. Saint-Petersburg: SPbTU Publisher; 2012.
[132] Borovkov AI, et al. Modern engineering education [In Russian]. Saint-Petersburg: SPbTU Publisher; 2012.
[133] Horikoshi K, Kato T. Theoretical study of the interparticle interaction of nanoparticles randomly dispersed on a substrate. J Appl Phys 2015; 117: 23117.
[134] Inan US, Marshall RA. Numerical electromagnetics: The FDTD method. Cambridge: Cambridge University Press; 2011: 316-326.
[135] Krietenstein B, et al. The perfect boundary approximation technique facing the challenge of high precision field computation. 19th Int Linear Accelerator Conf 1998: 860-862.
[136] Fritzen F, Bohlke T. Influence of the type of boundary conditions on the numerical properties of unit cell problems. Tech Mech 2010; 30(4): 354-363.
[137] Diebold S, et al. Modelling of transistor feeding structures based on electro-magnetic field simulations. 2012 Workshop on Integrated Nonlinear Microwave and Millimetre-wave Circuits 2012: 1-3.
[138] Sullivan DM. Electromagnetic simulation using the FDTD method. New York: Wiley-IEEE Press; 2013.
[139] Thoma P, Weiland T. A subgridding method in combination with the finite integration technique. 1995 25th European Microwave Conf 1995; 2: 1-4.
[140] Tian Y, et al. Numerical simulation of fiber-optic photoacoustic generator using nanocomposite material. J Comput Acoust 2013; 21(2): 1350002.
[141] Kurushin AA, Plastikov AN. Electrodynamics for CAD users [In Russian]. Moscow: "MEI" Publisher; 2011.
[142] Clemens M, Weiland T. Discrete electromagnetism with the finite integration technique. Progress in Electromagnetics Research 2001; 32: 65-87.
[143] Bankov SE, Kurushin AA. Electrodynamics and microwave technology for CAD users [In Russian]. Moscow: "IRE AN" Publisher; 2008.
[144] Pozar DM. Microwave engineering. 4th ed. Hoboken: John Wiley & Sons; 2012.

[145] Clemens M, Feigh S, Weiland T. Geometric multigrid algorithms using the conformal finite integration technique. IEEE Trans Magn 2004; 40(2): 1065-1078.
[146] Bondeson A, Rylander T, Ingelstron P. Texts in applied mathematics – Computational electromagnetics. New York: Springer; 2005p.
[147] Podoltsev AD, Kucherjavaya IN. Multiphysics simulation of electrical devices [In Russian]. Tehnichna Elektrodinamika 2015; 2: 3-15.
[148] Hameyer K, et al. The classification of coupled field problems. IEEE Trans Magn 1999; 35(3): 1618-1621.
[149] Bezzubceva MM, Volkov VS. Analytical review of application software packages for modeling energy processes in consumer energy systems of the agro-industrial complex [In Russian]. Mezhdunarodnyy Zhurnal Prikladnykh i Fundamental'nykh Issledovaniy 2015; 6(2): 191-195.
[150] Hoffmann J, et al. Comparison of electromagnetic field solvers for the 3D analysis of plasmonic nano antennas. Proc SPIE 2009; 7390: 73900J.
[151] Sarid D, Challener W. Modern introduction to surface plasmons: theory, mathematica modeling and applications. New York: Cambridge University Press; 2010.
[152] Wolfe C. Multiphysics: the future of simulation. ANSYS Advantage 2014; 8(2): 6-10.
[153] Paulsen M, et al. Simulation methods for multiperiodic and aperiodic nanostructured dielectric waveguides. Opt Quantum Electron 2017; 49(107): 106-120.
[154] Al-Mufti WM, Hashim U, Adam T. The state of the arts: simulation of nanostructures using COMSOL Multiphysics. Adv Mater Res 2013; 832: 206-211.
[155] Zhangyang X, et al. The effect of geometry parameters on light harvesting performance of GaN nanostructure arrays–a numerical investigation and simulation. Mater Res Express 2019; 7(1): 15009.
[156] Seth M, Ewusi-Annan E, Jensen L. Controlling the nonresonant chemical mechanism of SERS using a molecular photoswitch. Phys Chem Chem Phys 2009; 11: 7424-7429.
[157] Li JF, et al. Shelled-isolated nanoparticle-enhanced Raman spectroscopy. Nature 2010; 464: 392-395.
[158] Sidorov AN, et al. A surface-enhanced Raman spectroscopy study of thin graphene sheets functionalized with gold and silver nanostructures by seed-mediated growth. Carbon 2012; 50(2): 699-705.
[159] Herrera GM, Padilla AC, Hernandez-Rivera SP. Surface enhanced Raman scattering (SERS) studies of gold and silver nanoparticles prepared by laser ablation. Nanomaterials 2013; 3(1): 158-172.
[160] Mikitchuk AP, Kozadaev KV. Photostability of fiber-optic photoacoustic transducer based on silver nanoparticle layer. Semiconductors 2020; 54(14): 1836-1839. DOI: 10.1134/S1063782620140195.
[161] Goncharov VK, Kozadaev KV, Mikitchuk AP, Puzyrev MV. Synthesis, structural and spectral properties of surface noble metal nanostructures for fiber-optic photoacoustic generation. Semiconductors 2019; 53(14): 1950-1953. DOI: 10.1134/S1063782619140070.
[162] Girshova EI, Mikitchuk AP, Belonovski AV, Morozov KM, Kaliteevski MA. Prospects for using organic and metal−polymer materials in optoacoustic generators of ultrasound. Bulletin of the Russian Academy of Sciences: Physics 2022; 86(7): 833-836. DOI: 10.3103/S1062873822070140.
[163] Mikitchuk AP, Kozadaev KV. Photoacoustic generation with surface noble metal nanostructures. Semiconductors 2018; 52(14): 1839-1842. DOI: 10.1134/S106378261814018X.
[164] Nishijima Y, Rosa L, Juodkazis S. Surface plasmon resonances in periodic and random patterns of gold nano-disks for broadband light harvesting. Opt Express 2012; 20(10): 11466-11477.
[165] Pozar DM. Microwave engineering. John Wiley & Sons; 2012.
[166] Fritzen F, Bohlke T. Influence of the type of boundary conditions on the numerical properties of unit cell problems. Tech Mech 2010; 30(4): 354-363.
[167] Girshova EI, Mikitchuk AP, Belonovski AV, Morozov KM. Hybrid metal polymer as a potential active medium of an optoacoustic generator. Tech Phys Lett 2022; 48(2): 32-35. DOI: 10.21883/TPL.2022.02.52842.18948.
[168] Kreibig U, Vollmer M. Optical properties of metal clusters. Springer-Verlag; 1995.
[169] Mikitchuk AP, Girshova EI, Kugeiko MM. Thermophysical and mechanical properties of active membranes for photoacoustic generators of forced acoustic oscillations. Tech Phys Lett 2022; 48(4): 50-53. DOI: 10.21883/TPL.2022.04.53171.19089.
[170] Mikitchuk A, Kozadaev K. Comprehensive theoretical study of optical, thermophysical and acoustic properties of surface nanostructures with metallic nanoparticles for fiber-optic photoacoustic ultrasound transducers. Przeglad Elektrotechniczny 2020; 3: 129-137.

Authors' information

Alena Mikitchuk (b. 1989), graduated from Belarusian State University in 2012, defended her Ph.D. qualificative work in 2020. Works as Associate Professor of the Quantum Radiophysics and Optoelectronics department of Belarusian State University. Research interests: optoacoustics, computer optics, image analysis, image processing.
E-mail: *m.helenay@yandex.by* .

Elizaveta Ilinichna Girshova (b. 1991), graduated from Saint-Petersburg State University in 2016. Currently she works as an engineer in Research Center for Advanced Functional Materials and Laser Communication Systems. Research interests are nanophotonics, optoacoustics, light-matter interaction. E-mail: *ilinishna@gmail.com* .

Valentin Nikolaev (b. 1978), graduated from Peter the Great St. Petersburg Polytechnic University in 2001. He received his PhD in Physics degree from the University of Exeter, UK, in 2002 and his Candidate in Physics & Maths degree from Ioffe Institute, St. Petersburg, Russia in 2005. He worked as a researcher in University of York, Ioffe Institute and Submicron Heterostructures for Microelectronics Research and Engineering Center of the Russian Academy of Science. His current research interests include nanophotonics and optics of semiconductor nanostructures.
E-mail: *valia.nikolaev@gmail.com* .

Received September 13, 2022. The final version – February 20, 2023.